AD_____

AWARD NUMBER DAMD17-98-1-8060

TITLE: Contribution of the Receptor/Ligand Interaction Between CD44 and Osteopontin to Formation of Breast Cancer Metastases

PRINCIPAL INVESTIGATOR: Georg F. Weber, M.D., Ph.D.

CONTRACTING ORGANIZATION: Dana Farber Cancer Institute
Boston, Massachusetts 02115-6084

REPORT DATE: July 1999

TYPE OF REPORT: Annual

PREPARED FOR: U.S. Army Medical Research and Materiel Command
Fort Detrick, Maryland 21702-5012

REPORT DOCUMENTATION PAGE

Form Approved
OMB No. 0704-0188

1. AGENCY USE ONLY *(Leave blank)*	2. REPORT DATE	3. REPORT TYPE AND DATES COVERED
	July 1999	Annual (1 Jul 98 - 30 Jun 99)

4. TITLE AND SUBTITLE
Contribution of the Receptor/Ligand Interaction Between CD44 and Osteopontin to Formation of Breast Cancer Metastases

5. FUNDING NUMBERS
DAMD17-98-1-8060

6. AUTHOR(S)
Georg F. Weber, M.D., Ph.D.

7. PERFORMING ORGANIZATION NAME(S) AND ADDRESS(ES)
Dana Farber Cancer Institute
Boston, Massachusetts 02115-6084

8. PERFORMING ORGANIZATION REPORT NUMBER

9. SPONSORING / MONITORING AGENCY NAME(S) AND ADDRESS(ES)
U.S. Army Medical Research and Materiel Command
Fort Detrick, Maryland 21702-5012

10. SPONSORING / MONITORING AGENCY REPORT NUMBER

11. SUPPLEMENTARY NOTES

12a. DISTRIBUTION / AVAILABILITY STATEMENT
Approved for public release; distribution unlimited

12b. DISTRIBUTION CODE

13. ABSTRACT *(Maximum 200 words)*

Splice variants of the homing receptor CD44 may mediate metastasis formation by various tumors through interaction with the cytokine osteopontin which mediates cell attachment or migration. We have identified the mechanism of cell motility as a two-step process involving both major osteopontin receptors. We have further characterized the important involvement of osteopontin in delayed type immune responses which may have implications for tumor immunology. Future experiments will define CD44-dependent homing and invasion in vivo using our recently generated stably transfected tumor cells of various CD44 splice variants.

14. SUBJECT TERMS
Breast Cancer, Metastasis, Cytokines, Invasion

15. NUMBER OF PAGES
89

16. PRICE CODE

17. SECURITY CLASSIFICATION OF REPORT	18. SECURITY CLASSIFICATION OF THIS PAGE	19. SECURITY CLASSIFICATION OF ABSTRACT	20. LIMITATION OF ABSTRACT
Unclassified	Unclassified	Unclassified	Unlimited

FOREWORD

Opinions, interpretations, conclusions and recommendations are those of the author and are not necessarily endorsed by the U.S. Army.

NA Where copyrighted material is quoted, permission has been obtained to use such material.

NA Where material from documents designated for limited distribution is quoted, permission has been obtained to use the material.

NA Citations of commercial organizations and trade names in this report do not constitute an official Department of Army endorsement or approval of the products or services of these organizations.

✓ In conducting research using animals, the investigator(s) adhered to the "Guide for the Care and Use of Laboratory Animals," prepared by the Committee on Care and use of Laboratory Animals of the Institute of Laboratory Resources, national Research Council (NIH Publication No. 86-23, Revised 1985).

NA For the protection of human subjects, the investigator(s) adhered to policies of applicable Federal Law 45 CFR 46.

✓ In conducting research utilizing recombinant DNA technology, the investigator(s) adhered to current guidelines promulgated by the National Institutes of Health.

✓ In the conduct of research utilizing recombinant DNA, the investigator(s) adhered to the NIH Guidelines for Research Involving Recombinant DNA Molecules.

NA In the conduct of research involving hazardous organisms, the investigator(s) adhered to the CDC-NIH Guide for Biosafety in Microbiological and Biomedical Laboratories.

7-29-1999

PI - Signature Date

TABLE OF CONTENTS

INTRODUCTION

Splice variants of the homing receptor CD44 mediate metastasis formation by various tumors. Expression of the cytokine osteopontin has been associated with malignant potential of tumor cells. We have identified a novel receptor/ligand interaction between CD44 and osteopontin that mediates cell attachment or migration. Both molecules are subject to multiple posttranscriptional and pottranslational modifications and our data suggest that these alterations modulate binding. Organ-preference in metastasis formation may be based on specific recognition via homing receptors and modifications in CD44/osteopontin interaction may provide a potential molecular explanation. To assess why breast cancer metastasizes predominantly into bone, we are investigating modifications in both proteins that allow interaction.

BODY

Specific Aim 1: Identification of the posttranslational modifications in both proteins which are permissive for interaction.

A splice variant of CD44 (containing variant exon 6) is frequently expressed on malignant cells but not in the healthy adult organism. In our original identification of the CD44/osteopontin interaction (Weber et al. 1996) we had not dissected whether the osteopontin binding site on CD44 is located on the standard form or on any of the variant exons. We realized that the standard form does not bind this ligand and communicated that in a letter to the editor (Science 1998;282:243). This result was confirmed and extended by other investigators (Katagiri et al. 1999).

Tasks 1-3: To elucidate the mechanisms by which osteopontin mediates cell motility we have performed structure activity analysis of osteopontin and its receptors in macrophage migration and activation as model for metastatic spread. We find that an interaction between the C-terminal domain of osteopontin and the receptor CD44 induces macrophage chemotaxis via G-protein signalling, while engagement of integrin receptors by a non-overlapping N-terminal osteopontin domain induces cell spreading, mediated by PKC, and macrophage activation involving phosphatidylinositol as a secondary signal transduction component. Serine phosphorylation of the osteopontin molecule on specific sites is required for functional interaction with integrin but not CD44 receptors (Weber et al. 1999; see appendix).

Task 4: We attempted to define the consequences of interactions between CD44 and osteopontin in a modified Boyden chamber where the upper surface of the transmembrane was coated with matrigel to measure cell invasion. Those expreiments were entirely

unsuccessful. We now know that the presence of laminin (the major constitutent of matrigel) interferes with the effect of osteopontin on cell motility (we have made similar observations with regard to the laminin effect on osteopontin-mediated T-cell costimulation (Adler B, Ashkar S, Cantor H, Weber GF. 1999. Costimulation through adhesion molecules determines the response to ligation of the T-cell antigen receptor. Manuscript in preparation)). The identification of this laminin effect may potentially lead to novel treatment options for metastatic tumors.

Mice deficient in osteopotnin gene expression fail to develop delayed type hypersensitivity responses or Th1-driven autoimmunity after viral infection. These defective immune responses are associated with diminished production of the stimulatory cytokine IL-12 and excessive production of the inhibitory cytokine IL-10. A phosphorylation-dependent interaction between the N-terminal portion of osteopontin and its integrin receptor on macrophages leads to IL-12 expression, while a phosphorylation independent interaction of osteopontin with CD44 inhibits IL-10 expression (Ashkar et al. 1999; see appendix). The CD44-dependent inhibition of IL-10 expression by macrophages has potential implications for tumor immunology because tumor-derived osteopontin may have a deletion in the N-terminal portion of the molecule (Kiefer et al. 1989; Ashkar, personal communication) so that the Th1-inducing ligation of integrins on macrophages is prevented while engagement of macrophage CD44 inhibits the Th2-inducing secretion of IL-10 with consequent immune suppression.

Based on the immunomodulatory effect of osteopontin, we have designed candidate peptide drugs that selectively interfere with receptor binding to either CD44 or integrin $\alpha_v\beta_3$ (patent pending; see appendix).

Cancers of particular tissue origin show consistent preference for specific target organs to spread to. This topology of metastasis formation is mediated by the potpourri of homing receptors on the tumor cell surface and their ligands and is widely believed to have its physiologic correlate in morphogenesis during embryonic

development. Unexpectedly, knockout mice in which individual genes known to participate in tumor spread were disrupted turned out to be fertile and developmentally normal. The defects observed in the relevant gene targeted mice are impairments of various features of stress responses. Metastasis-associated gene products have several features in common. They comprise a set of developmentally non-essential genes which physiologically mediate stress responses, including inflammation, wound healing, and neovascularization. Recognition of topology is encoded in the surface molecules of immune cells and organ preference by cancer may be derived from a process which immune cells use to target their responses. Metastasis-associated gene products therefore constitute a unique and essential group of cancer related biomolecules. We conclude that metastasis formation is a process that mimicks macrophage behavior (Weber/Ashkar 1999; see appendix).

Specific Aim 2: Investigation into the roles of CD44 and osteopontin in metastasis formation.

Task 5: We have recently transfected cells that do not express endogenous CD44 (the Balb/c derived leukemia cell line S49 as well as osteosarcoma cells derived from a mouse with mutant p53 and gene-knockout of CD44 that was bred and raised in our laboratory) with retroviral vector containing GFP and, in a separate open reading frame, no gene, CD44v4-v10, CD44v7-v10, or CD44v8-v10 (Figure 1). We will use these cell lines in in vitro and in vivo experiments.

Figure 1: S49 cells transfected with constructs of various CD44 variants. Successfully transfected cells display endogenous greeen fluorescence (FL1) due to GFP in the vector. In addition, the cells were stained with PE-conjugated anti-CD44 antibody (FL2).

24Jun99 20:02:53
f-cd4/p-cd44/cyc3g11
Z0008253
S49_44-pe
24 seconds, 6516 events
Stop Count: 5000 events, histogram 4

4: A

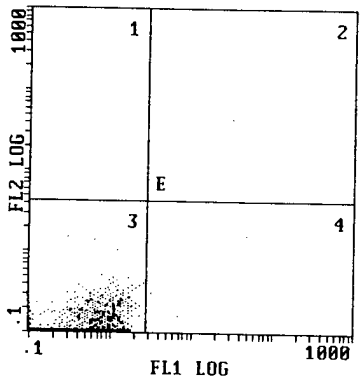

24Jun99 19:48:10
f-cd4/p-cd44/cyc3g11
Z0008242
Vec_44-pe
64 seconds, 5726 events
Stop Count: 5000 events, histogram 4

4: A

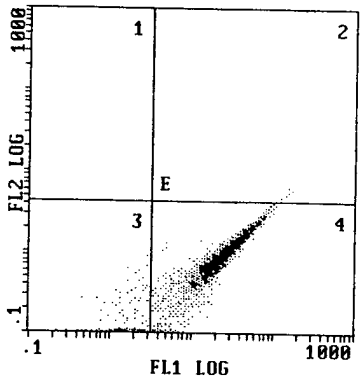

10

24Jun99 19:50:53
f-cd4/p-cd44/cyc3g11
Z0008244
V4_44-pe
48 seconds, 6266 events
Stop Count: 5000 events, histogram 4

4: A

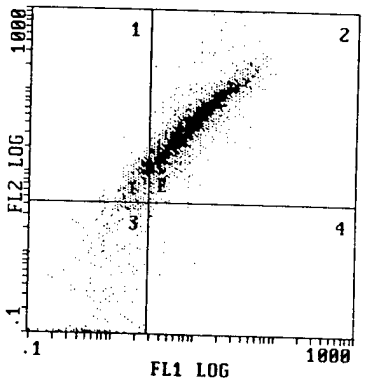

24Jun99 19:57:59
f-cd4/p-cd44/cyc3g11
Z0008248
V7_44-pe
12 seconds, 6209 events
Stop Count: 5000 events, histogram 4

4: A

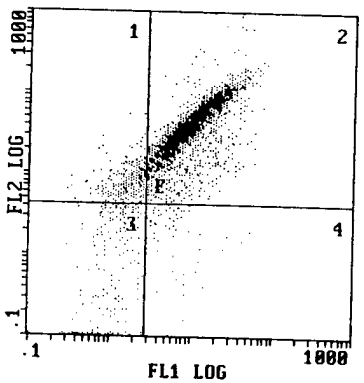

24Jun99 20:01:11
f-cd4/p-cd44/cyc3g11
Z0008251
V8_44-pe
22 seconds, 12542 events
Stop Count: 5000 events, histogram 4

4: A

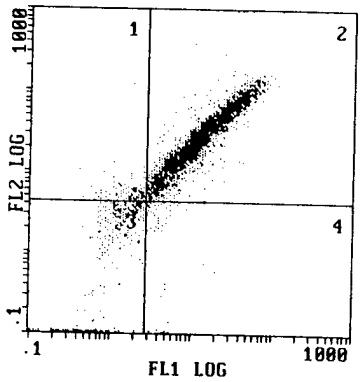

KEY RESEARCH ACCOMPLISHMENTS

* structure-activity analysis of osteopontin in cell migration and activation

* identification of suppression of IL-10 expression by macrophages as consequence of interaction between osteopontin and CD44 which may have implications for tumor immunology

* theoretical consideration regarding metastasis formation as mimickry of macrophage activation

* cloning and transfection of several CD44 splice variants into $CD44^{-/-}$ tumor cells.

REPORTABLE OUTCOMES

Ashkar S, Weber GF, Panoutsakopoulou V, Sanchirico ME, Zawaideh S, Rittling S, Denhardt DT, Glimcher MJ, Cantor H. 1999. The Eta-1/Opn cytokine is an essential molecular bridge to type 1 (cell-mediated) immunity. Manuscript under revision.

Weber GF, Zawaideh S, Kumar VA, Glimcher MJ, Cantor H, Ashkar S. 1999. Phosphorylation-dependent interaction of osteopontin with its receptors regulates macrophage migration and activation. Manuscript in preparation.

Weber GF, Ashkar S. 1999. The genes that make cancer metastasize. Manuscript in preparation.

Ashkar S, Weber GF (inventors). Biosynthetic immunomodulatory molecules and uses therefor. U.S. patent pending.

CONCLUSIONS

We have further delineated the functional consequences of the interactions between osteopontin and its receptors. We have identified the mechansim of cell motility as a two-step process involving both major osteopontin receptors. These may be the molecular underpinnings of tumor invasion. We have further characterized the important involvement of osteopontin in delayed type immune responses which may have implications for tumor immunology. Future experiments will define CD44-dependent homing and invasion in vivo using our recently generated stably transfected tumor cells of various CD44 splice variants.

REFERENCES

Katagiri YU, Sleeman J, Fujii H, Herrlich P, Hotta H, Tanaka K, Chikuma S, Yagita H, Okumura K, Murakami M, Saiki I, Chambers AF, Uede T. CD44 variants but not CD44s cooperate with beta1-containing integrins to permit cells to bind to osteopontin independently of arginine-glycine-aspartic acid, thereby stimulating cell motility and chemotaxis. Cancer Res. 1999;59:219-226.

Kiefer MC, Bauer DM, and Barr PJ. The cDNA and derived amino acid sequence for human osteopontin. Nucl. Acid Res. 1989;17:3306.

Weber GF, Ashkar S, Glimcher MJ, Cantor H. Receptor-ligand interaction between CD44 and osteopontin (Eta-1). Science 1996;271:509-512.

APPENDICES

The Eta-1/Opn Cytokine is an Essential Molecular Bridge to Type 1 (Cell-Mediated) Immunity

Samy Ashkar[1*], Georg F. Weber[2,3*], Vassiliki Panoutsakopoulou[2,4], Marie E. Sanchirico[2,4], Samer Zawaideh[1], Susan R. Rittling[5], David T. Denhardt[5], Melvin J. Glimcher[1] and [*]Harvey Cantor[2,4].

[1]Laboratory for Skeletal Disorders and Rehabilitation, Department of Orthopedic Surgery, Children's Hospital, Harvard Medical School, 300 Longwood Avenue, Boston, MA 02115; [2]Department of Cancer Immunology & AIDS, Dana-Farber Cancer Institute Departments of Medicine[3] and Pathology[4], Harvard Medical School, 44 Binney Street, Boston, MA 02115; [5]FAS-Division of Life Sciences, Rutgers University, 604 Allison Road, New Jersey 08854

[*] These authors contributed equally to this project.

[*] Address correspondence to: Harvey Cantor, 44 Binney Street, Boston MA 02115; (617) 632-3348; 4630-FAX; Harvey_Cantor@DFCI.harvard.edu

ABSTRACT

Cell-mediated (Type 1) immunity associated with Th1 cells is necessary for immune protection against intracellular pathogens and, when excessive, can mediate organ-specific autoimmune destruction. Mice deficient in Eta-1/Opn gene expression fail to develop DTH responses or Th1-driven autoimmunity after viral infection. These defective immune responses are associated with diminished production of the stimulatory cytokine IL-12 and excessive production of the inhibitory cytokine IL-10. A phosphorylation-dependent interaction between the N-terminal portion of Eta-1/Opn and its integrin receptor on macrophages leads to IL-12 expression, while a phosphorylation independent interaction of Eta-1/Opn with its CD44 receptor inhibits IL-10 expression. These findings identify Eta-1/Opn as a key cytokine that sets the stage for efficient Type 1 immune responses through differential engagement of its receptors on macrophages.

Development of cell-mediated (Type 1) immunity is essential for protection against the growth of both infectious pathogens and tumor cells. Although microbial infection (1) and cellular necrosis (2) can efficiently stimulate Type 1 immune responses, the molecular elements that dictate this form of immunity are not well understood. An early and essential step in this process is the T cell-dependent migration and activation of macrophages/dendritic cells to the site of infection. Production of IL-12 by macrophages/dendritic cells and reception of the IL-12 signal by CD4 cells (3) are subsequent critical steps in this process. Although an interaction between CD40 ligand on activated T cells and CD40 on macrophages can induce IL-12 expression (4) this interaction also induces the inhibitory IL-10 cytokine and may not suffice for induction of IL-12 *in vitro* (5) or for a sustained IL-12 response to viral infection *in vivo* (6).

A gene product that may play a critical role in Type 1 responses is the T cell cytokine Eta-1 (for Early T-lymphocyte activation-1), also known as osteopontin (Opn) (7). Eta-1/Opn is the most abundantly expressed mRNA transcript after activation of CD4 cells and interacts with macrophages to mediate genetic resistance to several intracellular pathogens (7, 8). Resistance to *Rickettsial* infection is characterized by vigorous induction of Eta-1/Opn that promotes an early monocyte influx into infected sites and acquisition of macrophage bacteriocidal activity. Susceptibility to *Rickettsial* infection, on the other hand, reflects delayed and weak Eta-1/Opn responses and is characterized by a paucity of macrophages at sites of infection (7, 9). T cell expression of Eta-1/Opn is also associated with granuloma formation in tuberculosis and silicosis (10) and may contribute to chronic glomerulonephritis (11). In view of its association with these

and other cell-mediated inflammatory reactions (12), we asked whether the Eta-1/Opn gene product represented an essential component of Type 1 immune responses.

Infection by herpes simplex virus-1 (HSV-1) is associated with the development of HSV-1-specific delayed-type hypersensitivity (DTH) reactions upon restimulation with virus (13). We investigated whether mice deficient in Eta-1/Opn gene expression secondary to targeted gene mutation (14) can mount DTH responses to HSV-1. Eta-1/Opn$^{-/-}$ mice infected by HSV-1 ($4x10^6$ pfu via the cornea) fail to develop a significant DTH response after footpad challenge with 10^5 pfu HSV-1, in contrast to the strong DTH response of Eta-1/Opn$^{+/+}$ controls (Figure 1A). Although the proportions of T cell subsets in the thymus and peripheral lymphoid tissues of unchallenged Eta-1/Opn$^{-/-}$ mice are not abnormal, defective anti-viral DTH responses might reflect subtle alteration in lymphocyte/macrophage development. We therefore tested the effects of acute depletion of Eta-1/Opn with a neutralizing antibody. Administration of anti-Eta-1/Opn antibody LF-123 (15) but not control rabbit immunoglobulin immediately before and repeatedly after HSV-1 infection efficiently inhibited the DTH response upon rechallenge (**Figure** 1B).

Corneal HSV-1 infection can lead to the development of Herpes Simplex Keratitis (HSK), a destructive autoimmune inflammatory reaction initiated by CD4 cells that recognize a viral peptide mimic of a murine corneal self-antigen (16). The development of HSK in mice lacking T cells (e.g., Rag-2$^{-/-}$ mice) requires reconstitution with CD4 cells immediately before HSV-1 corneal infection and is inhibited by local administration of IL-10 (16,17). Since Eta-1/Opn$^{-/-}$ mice fail to develop HSV-1-specific DTH, we investigated whether they displayed impaired HSK. Within 10-14 days after corneal HSV-1 infection, about 65% of control (Eta-1/Opn$^{+/+}$)

mice developed HSK, while HSV-1-infected Eta-1/Opn$^{-/-}$ mice did not display significant levels of this disease (Figure 1C). This did not reflect a general impairment of the immune system in these mice since the extent of T cell expansion followed by apoptosis after superantigen (SEB) injection was indistinguishable from wild-type mice (not shown).

We analyzed cells from lymphoid tissues of mice after corneal HSV-1 infection. Although cells from the draining lymph nodes of virus-infected Eta-1/Opn$^{-/-}$ and Eta-1/Opn$^{+/+}$ mice respond equally well to HSV-1 according to ^{3}H-thymidine incorporation after viral restimulation *in vitro*, they differed conspicuously according to their cytokine profiles. Cells from Eta-1/Opn$^{-/-}$ mice produced high levels of IL-10 and IL-4 but markedly reduced levels of IL-12 compared with Eta-1/Opn$^{+/+}$ controls (Figure 1D), and splenic macrophages from virus-infected Eta-1/Opn$^{+/+}$ but not Eta-1/Opn$^{-/-}$ mice continued to produce IL-12 ten days after infection. This cytokine profile suggests that Eta-1/Opn expression normally may imprint the *in vivo* ratio of IL-12 and IL-10 cytokines that in turn dictates Type 1 immunity.

To define the effect of Eta-1/Opn on IL-10 and IL-12 production by macrophages *in vitro*, we incubated resident peritoneal macrophages with increasing concentrations of purified Eta-1/Opn in serum-free medium (Figure 2A). This resulted in the secretion of as much as 400 pg/ml of IL-12 at 48 h while IL-10 production was not detected (Figure 2A,B). Eta-1/Opn-dependent induction of IL-12 secretion from macrophages was not due to contamination with endotoxin: Limulus amoeboid lysate assay (Sigma, St. Louis MO) indicated that purified Eta-1/Opn contained less than 1ng/g endotoxin. Moreover, quantities of endotoxin that escape detection in the limulus ameboid lysate assay do not contribute to biologic activity of Eta-1/Opn because

the IL-12 response of macrophages derived from C3H.HeJ mice (which are defective in endotoxin receptor-mediated signalling) was not impaired compared to other strains (Figure 3C). The failure of Eta-1/Opn to induce IL-10 was somewhat surprising since other cytokines that activate macrophages, including TNFα, IL-1,-2,-3,-6 (18), all stimulate IL-10 secretion, and LPS stimulation of these resident peritoneal macrophages induced both IL-12 (about 250 pg/ml) and IL-10 (about 100 pg/ml) (Figure 2B). Further analysis showed that Eta-1/Opn actively suppresses the IL-10 response of resident peritoneal macrophages since IL-4-dependent induction of macrophage IL-10 was inhibited by the addition of Eta-1/Opn and this effect was not altered by anti-IL-12 neutralizing antibody, suggesting a direct mode of action (Figure 2C).

The interaction of Eta-1/Opn with macrophages is mediated through two functional receptors. Engagement of CD44 mediates chemotactic migration (19) and interaction with $\alpha_v\beta_3$ integrin causes haptotaxis, adhesion and spreading (20). We asked which receptor was responsible for the regulation of macrophage cytokine production by Eta-1/Opn. Induction of IL-12 is inhibited by GRGDS peptide (but not GRGES peptide), by anti-integrin β_3 but not by anti-CD44 antibody. Macrophages from CD44$^{-/-}$ mice (21) display an unimpaired IL-12 response. To further characterize the RGD-dependent interaction between the macrophage β_3-containing integrin receptor and Eta-1/Opn, we analyzed fragments from a Lys-C digest and found that a proteolytic fragment from the N-terminal portion of Eta-1/Opn which contains the integrin binding site (termed NK10) (22) is sufficient to induce macrophage IL-12 expression (Figure 3A). In contrast to IL-12 induction, inhibition of IL-10 depends on engagement of the CD44 receptor: Eta-1/Opn-dependent inhibition of IL-10 is blocked by anti-CD44 but not anti-integrin β_3

antibody and macrophages from CD44 mice are resistant to Eta-1/Opn inhibition of the IL-10 response (Figure 3A,B).

Eta-1/Opn is secreted in nonphosphorylated and phosphorylated forms (23). Phosphorylation may allow Eta-1/Opn to associate with the cell surface rather than the extracellular matrix (24) through a contribution to integrin binding. In contrast, serine phosphorylation of recombinant Eta-1/Opn is not required for CD44-dependent interactions leading to chemotactic migration (19). We investigated whether phosphorylation of Eta-1/Opn might affect its ability to regulate IL-12/IL-10 expression. Dephosphorylated purified naturally-produced Eta-1/Opn abolishes IL-12 stimulatory activity; phosphorylation of recombinant Eta-1/Opn at specific sites restores activity (Figure 4A). Although recombinant Eta-1/Opn lacking phosphate groups cannot induce IL-12, this molecule retains inhibitory activity for the macrophage IL-10 response (Figure 4B). There is abundant evidence that phosphorylation can regulate the biological activity of intracellular enzymes and their substrates. These results indicate that serine phosphorylation can also provide molecular information that regulates the biological activity of a secreted protein.

We have identified expression of Eta-1/Opn by activated T cells represents an essential molecular link between T cell recognition and cell-mediated immunity. These findings fill a logical gap in our understanding of the cellular and molecular mechanisms that enhance Type 1 immune responses. Although downregulation of CD40 ligand expression by γ-IFN and soluble CD40 occurs within 24 hours after viral infection, IL-12 is detected in serum over the next 7-10 days (6). Our experiments suggest that replacement of the CD40L signal by Eta-1/Opn is essential to potentiate the IL-12 response and allow Type 1 immunity. A critical feature of the

regulatory effects of Eta-1/Opn is its ability to engage an IL-10 inhibiting receptor (25) and thus up-regulate production of Type 1 cytokines other than IL-12. Although mice deficient in IL-12 gene expression develop fewer γ-IFN-producing T cells following immunization, they retain the ability to mount a reduced but significant DTH response, the cellular signature of Type 1 immunity (26). Concomitant inhibition of IL-10 expression by Eta-1/Opn may allow increased production of Type 1 cytokines that together give rise to efficient development of cell-mediated immunity. Eta-1/Opn imprinting of the IL-12-IL-10 response after appropriate peptide stimulation (27) may also increase the likelihood of autoimmune sequelae, as judged from studies of murine EAE (28).

Regulated expression of two early cytokine checkpoints in the development Type 1 or Type 2 immune responses by Eta-1/Opn also forms a potential basis for new therapeutic approaches to several diseases. Eta-1/Opn analogs that mediate CD44-dependent inhibition of IL-10 may inhibit sepsis in burn patients (29) while antagonists of this pathway may ameliorate bacterial arthritis (30). Engineered forms of Eta-1/Opn that imprint Type 1 responses following immunization may be valuable components of viral and cancer vaccines.

References & Notes:

1. E. R. Unanue, *Immunol. Revs.* **158**, 11 (1997); R. Medzhitov, C. Janeway, *Seminars in Immunol.*, **10**, 351-353 (1998).

2. P. Matzinger, *Seminars in Immunol.*, **10**, 399 (1998).

3. C. M. Scheicher, M. Mehlig, H. P. Dienes, K. Reske, *Eur. J. Immunol.*, **25**, 1566 (1995); S. E. Macatonia, *et al*, *J. Immunol.*, **154**, 5071 (1995); K. M. Murphy, *Curr. Opin. Immunol.* **10**, 226 (1998).

4. F. Koch, *et al*, *J. Exp. Med.*, **184**, 741 (1996); A. O'Garra, *Immunity*, **8**, 275 (1998).

5. F. Ria, G. Penna, L. Adorini, *Eur. J. Immunol.*, **28**, 2003 (1998).

6. M. D. Sharma, M. L. de Moraes, F. Zavala, C. Pontoux, M. Papiernik, *J. Immunol.*, **161**, 5357 (1998).

7. R. Patarca, *et al*, *J. Exp. Med.*, **170**, 145 (1989).

8. R. Patarca, R. A. Saavedra, H. Cantor, *Crit. Revs. Immunol.*, **13**, 225 (1993).

9. T. J. Jerrells, J. V. Osterman, *Infect. Immun.*, **31**, 1014 (1981).

10. G. J. Nau, *et al*, *Proc. Natl. Acad. Sci. USA*, **94**, 6414 (1997); I. I. Singer, *et al*, *J. Clin. Invest.*, **95**, 2178 (1995); A. W. O'Regan, G. L. Chupp, J. A. Lowry, M. Goetschkes, N. Mulligan, J. S. Berman, *J. Immunol.*, **162**, 1024 (1999).

11. X. Q. Yu, *et al*, *Proc. Assoc. Amer. Phys.*, **110**, 50 (1998).

12. X. Wang, *et al*, *J. Neurosci.*, **18:**, 2075 (1998); C. M. Giachelli, L. Liaw, C. E. Murry, S. M. Schwartz, M. Almeida, *Ann. NY Acad. Sci.*, **760**, 109 (1995).

13. C. S. Foster, *et al*, *Clin. Immunol. Immunopathol.*, **40**, 313 (1986).

14. S. R. Rittling, *et al*, *J. Bone & Min. Res.*, **13**, 1101 (1998).

15. L. W. Fisher, J. T. Stubbs, M. F. Young, *Acta Orthop. Scand.*, **66**, 61 (1995).

16. A. C. Avery, *et al*, *Nature*, **376**, 431 (1995); Z-S. Zhao, F. Granucci, L. Yeh, P. A. Schaffer, H. Cantor, *Science*, **279**, 1344 (1998).

17. M. Daheshia, N. Kuklin, S. Kanangat, E. Manickan, B. T. Rouse, *J. Immunol.*, **159**, 1945 (1997).

18. P. Stordeur, L. Schandane, P. Durez, C. Gerard, M. Goldman, T. Velu, *Mol. Immunol.*, **32**, 233 (1995); P. Stordeur, M. Goldman, *Int'l Revs. Immunol.*, **16**, 501 (1998).

19. G. F. Weber, S. Ashkar, M. J. Glimcher, H. Cantor, *Science*, **271**, 509 (1996).

20. R. P. Singh, R. Patarca, J. Schwartz, P. Singh, H. Cantor, *J. Exp. Med.*, **171**, 1931 (1990); L. Liaw, *et al*, *J. Clin. Invest.*, **95**, 713 (1995); M. Sato, M. K. Sardana, W. A. Grasser, V. M. Garsky, J. M. Murray, R. J. Gould, *J. Cell Biol.*, **111**, 1713 (1990).

21. R. Schmits, J. Filmus, N. Gerwin, et al, *Blood*, **90**, 2217 (1997).

22. Recombinant GST-Eta-1/Opn fusion protein was derived from E. coli, digested with factor Xa, and purified by affinity chromatography as described (S. Ashkar, M. J. Glimcher, R. A. Saavedra, *Biochem. Biophys. Res. Comm.*, **194**, 274 [1993]; S. Ashkar, D. B. Teplow, M. J. Glimcher, R. A. Saavedra, *Biochem. Biophys. Res. Comm.*, **191**, 126 [1993]). Native Eta-1/Opn was isolated from MC3T3E1 cells or Ar5v T cells. Cells were grown in defined media (consisting of DME/H12 supplemented with pyruvate, insulin, transferrin, selenium and ethanolmine) in 5% CO_2 at 37°C, concentrated PBS using a Millipore tangential flow system applied to Millipore LC100 equipped with a DEAE-Memsep 1000 cartridge and developed in a discontinuous gradient of 0 to 1 M NaCl in phosphate buffer, pH 7.4. Eta-1/Opn-containing fractions were pooled (the major Eta-1/Opn peak eluted at 0.26 M salt), concentrated by ultrafiltration,

chromatofocused on mono P columns (Pharmacia) at pH 8.2, developed with polybuffer 74 (Pharmacia) and the major Eta-1/Opn fraction eluted from monobeads at pH 4.6. The protein was judged pure by several criteria including SDS electrophoresis and amino acid sequence analysis (both N-terminal and internal peptide analysis). Mass spectroscopic analysis revealed a peak centered around a mass of 35,400 daltons that was highly phosphorylated (11 mols of phosphate/mol of protein), O-glycosylated but not N-glycosylated, and no measurable sulfate. Partial tryptic, chemotryptic or Asp-N endopeptidase digestion of Eta-1/Opn did not result in isolation of an active peptide, however, a 10 kD fragment was isolated from a Lys-C digest that had the N-terminal sequence QETLPSN, was predicted to terminate at the thrombin cleavage site, and contained approximately 5 mols of phosphate/mol of peptide at seven potential phosphorylation sites.

23. T. Kubota, *et al*, *Biochem. Biophys. Res. Comm.*, **162**, 1453 (1989); A. F. Chambers, E. I. Behrend, S. M. Wilson, D. T. Denhardt, *Anticancer Res.*, **12**, 43 (1992); E. S. Sorensen, T. E. Petersen, *Biochem. Biophys. Res. Comm.*, **198**, 200 (1994); H. Salih, S. Ashkar, L. C. Gerstenfeld, M. J. Glimcher, *J. Biol. Chem.*, **272**, 13966 (1997).

24. M. Nemir, M. W. DeVouge, B. B. Mukherjee, *J. Biol. Chem.*, **264**, 18202 (1989); B. Ek-Rylander, M. Flores, M. Wendel, D. Heinegard, G. Andersson, *J. Biol. Chem.*, **269**, 14853 (1994).

25. L. L. Lanier, *Annu. Rev. Immunol.* **16**, 359 (1998).

26. J. Magram, *et al*, *Immunity*, **4**, 471 (1996).

27. S. L. Constant, K. Bottomly, *Annu. Rev. Immunol.* **15**, 297 (1997).

28. B. M. Segal, B. K. Dwyer, E. M. Shevach, *J. Exp. Med.*, **187**, 537 (1998).

29. A. Lyons, J. L. Kelly, M. L. Rodrick, J. A. Mannick, J. A. Lederer, *Ann. Surg.*, **226**, 450 (1997); J. L. Kelly, A. Lyons, C. C. Soberg, J. A. Mannick, J. A. Lederer, *Surgery*, **122**, 146 (1997).

30. Z. Yin, *et al*, *Arth. Rheum.*, **40**, 1788 (1997).

31. *In vitro* stimulation of lymph node cells and splenic macrophages. The right superficial cervical draining lymph nodes of Eta-1/Opn$^{-/-}$ mice and their Eta-1/Opn$^{+/+}$ controls were harvested 15 days after infection of the right eye with $4x10^6$ pfu HSV-1 (KOS). Cells from these lymph nodes ($2x10^6$) were incubated in the presence of $4x10^7$ pfu UV-inactivated HSV-1 (KOS). Supernatants were harvested 48 h later and IL-10 and IL-12 p40 cytokine levels were measured by sandwich ELISA using OptIEA antibody sets (Pharmingen, La Jolla CA). IL-4 was measured after stimulation of draining lymph node cells by plate-bound anti-CD3.

32. Resident peritoneal macrophages were obtained by peritoneal lavage with 2x10 ml PBS. Contaminating red cells were eliminated by hypotonic lysis with ACK buffer. Cells were

incubated 10^5/100 μl in 96-well plates and non-adherent cells were washed off after 2 h. The macrophages were stimulated with 5 nM Eta-1/Opn, 30 ng/ml LPS, or 500 U/ml recombinant IL-4 or as indicated. Supernatant was withdrawn at the indicated time points for analysis of IL-10 or IL-12 p70 using commercial ELISA kits (R & D Systems). At the end of the incubation, the cells were tested for viability by propidium iodide incorporation and their purity was confirmed by staining with fluorescence-conjugated anti-Mac1 antibody. Blocking anti-IL-12 antibody was purchased from R & D Systems, Minneapolis, MN, blocking anti-integrin β_3 antibody was obtained from Pharmingen (JF Schultz, DR Armant. J. Biol. Chem. 1995:270:11522) and the anti-CD44 antibody KM81 was purified from ATCC hybridoma TIB 241 and has been shown previously to block the interaction of CD44 and Eta-1/Opn (19).

33. Dephosphorylation of Eta-1/Opn. 5 mg of purified Eta-1/Opn was dephosphorylated using 6 units (60 units/mg) type II potato acid phosphatase (Sigma) according to a published procedure (S. Ashkar *et al*, *Biochem.Biophys. Acta* 191, 126 [1993]). Briefly, Eta-1/Opn (5 mg) was incubated with 6 U of acid phosphatase in 20 mM phosphate buffer pH 4.8 at 37°C for 2 h. After adjusting the pH to 8.2, dephosphorylated protein was applied to a chromatofocusing column and the major peak eluted at a pH of 5.1; amino acid analysis of the protein revealed a phosphate content of less than 1 mol/mol protein. Phosphorylation of rEta-1/Opn: GST-Eta-1/Opn (5 mg) was phosphorylated as described (22; S. Ashkar, J. L. Schaffer, E. Salih, L. C. Gerstenfeld, M. J. Glimcher, *Ann. NY Acad. Sci.*, **760**, 296 [1995]). Briefly, 10 μg of Golgi kinase and 5 mg purified GST-Eta-1/Opn were incubated for 2 h before passage thorugh a GSH-Sepharose column

and elution from GSH-Beads with 100 U of factor Xa (22). The eluate was applied to a chromatofocusing column and eluted from the resin with polybuffer 74 (22). The major peak eluted at pH 4.6 and phospho-amino acid analysis of the recovered protein revealed a phosphoserine content of 16 mol of phosphate/mol protein and 0.8 mols of phosphothreonine/mol protein.

34. Supported in part by National Institutes of Health (NIH) research grant AI12184 to HC; NIH grant CA76176 and Department of Defense breast cancer grant BC972625 to GFW; grants from Biomorphics Inc., and a career development grant from Children's Hospital, Boston to SA; and National Institutes of Health grant AR34078 to MJG. SZ was supported by a grant from the Fullbright Foundation. Research at Rutgers developing the OPN knockout mice was supported by grants AR44434 to DTD and CA72740 to SRR. All experimentation involving animals was in accordance with Dana-Farber Institutional Guidelines. We thank T.W. Mak for $CD44^{-/-}$ mice and A. Angel and L. Lagasse for assistance in the preparation of the manuscript.

LEGENDS TO FIGURES

Figure 1.

Eta-1/Opn is essential for Type 1 immune responses to herpes simplex virus-1 (HSV-1).

A. Defective HSV-1-specific DTH responses in Eta-1/Opn$^{-/-}$ Mice. (C57Bl/6x129)F_1 with or without targeted disruption of the Eta-1/Opn gene were infected in the right eye with $4x10^6$ pfu HSV-1 (KOS) and challenged five days later in the left footpad with $1x10^5$ pfu of UV-inactivated HSV-1 (KOS) (13). The right (control, □) and left (HSV-1, ■) footpads of each mouse were measured 24 h later using a micrometer. Each data point represents the mean and standard error of three mice/group.

B. Inhibition of the anti-HSV-1 DTH response by acute depletion of Eta-1/Opn. The neutralizing antibody LF-123 (○) (15) or control normal rabbit serum (●) were injected at 25 μg per dose per day starting from day -2. On day 0, mice were infected with HSV-1 (KOS) and rechallenged five days later. The right and left footpads of each mouse were measured 24 h after rechallenge and specific swelling (left vs. right footpad) is shown.

C. Eta-1/Opn$^{-/-}$ mice are resistant to the development of HSK in comparison to Eta-1/Opn$^{+/+}$ controls. The right eyes of Eta-1/Opn$^{-/-}$ (○) and Eta-1/Opn$^{+/+}$ (●) mice were infected with $4x10^6$ pfu of HSV-1 (KOS) and disease was assessed on days 11 and 14 after infection as described (16). The severity of clinical stromal keratitis was scored based on the degree of corneal opacity; $\leq$25% of cornea, 1; $\leq$50%, 2; $\leq$75%, 3; 75-100%, 4. Each point represents at least 16 mice and is the mean of three independent experiments. **D.** Differential cytokine profile of draining lymph node cells and splenic macrophages from Eta-1/Opn$^{+/+}$ or Eta-1/Opn$^{-/-}$ mice after infection with HSV-1. Cytokine levels after restimulation of draining lymph node

cells (from mice 15 days after HSV-1 infection in vivo) by $4x10^7$ pfu UV-inactivated HSV-1 using 48 h supernatants were determined by ELISA (31). Eta-1/Opn$^{-/-}$ mice display high IL-12 and low IL-10 responses typical of Type 1 immunity, while lymph node cells from Eta-1/Opn$^{-/-}$ mice produce little IL-12 but high levels of IL-10 and IL-4. Similarly, splenic macrophages from the Eta-1/Opn$^{+/+}$ but not Eta-1/Opn$^{-/-}$ mice (10 days after HSV-1 infection) secrete high levels of IL-12. The proliferative response of lymph node cells from HSV-1-infected Eta-1/Opn$^{+/+}$ and Eta-1/Opn$^{-/-}$ mice measured by ^{3}H-thymidine incorporation at 72 h was $20.9x10^3$ and $18.7x10^3$ cpm, respectively.

Figure 2.

Differential regulation of macrophage IL-12 and IL-10 responses by purified Eta-1/Opn.

A. Dose-dependent induction of IL-12 secretion, but not IL-10 secretion, from macrophages by Eta-1/Opn. Resident peritoneal macrophages obtained from C57BL/6 mice (32) were incubated for 48 h ($5x10^5$/ml) with purified Eta-1/Opn (22) and levels of IL-10 and IL-12 p75 in the supernatant were determined by ELISA. Assays were performed in quadruplets and each point represents the mean and standard error of three independent experiments.

B. Time course of IL-12 p75/IL-10 expression by resident peritoneal macrophages ($5x10^5$/ml) after incubation with 5 nM Eta-1/Opn or 30 ng/ml LPS or 500 U/ml IL-4. While LPS induces secretion of IL-12 and IL-10, and while IL-4 predominantly causes production of IL-10, Eta-1/OPN selectively leads to secretion of IL-12. Assays were performed in quadruplets and each data point represents the mean and standard error of two independent experiments.

C. Inhibitory effects of Eta-1/Opn on macrophage IL-10 production. Macrophages were activated with IL-4 (500 U/ml x 1 hour) before addition of Eta-1/Opn (5 nM) for an additional

48 h and consecutive measurement of IL-12 and IL-10 by ELISA. In some groups, anti-IL-12 antibody was added at a final concentration of 2 μg/ml. Eta-1/Opn inhibits IL-4 induced secretion of IL-10 in a manner that is unaffected by the presence of anti-IL-12 antibody. Assays were performed in quadruplets and each point represents the mean and standard error of two independent experiments.

Figure 3.

Induction of IL-12 and inhibition of IL-10 are mediated by distinct receptors.

A. Secretion of IL-12 by macrophages (32) is mediated by a 10 kD peptide (NK10) derived from the N-terminal fragment of Eta-1/Opn (NT) and is inhibited by a blocking anti-integrin β_3 antibody (1 μg/ml), but is unaffected by antibody to CD44 (1 μg/ml).

B. IL-4-dependent induction of IL-10 production is inhibited by Eta-1/Opn. The inhibition is reversed by anti-CD44 antibody but not by anti-integrin β_3 antibody.

C. Secretion of IL-12 in response to Eta-1/Opn is not impaired in macrophages from mice that are deficient in the CD44 gene and cells from C3H.HeJ mice which do not respond to endotoxin display the same levels of induction as control mice. Conversely, while the inhibition of IL-10 secretion is not affected in C3H.HeJ mice (which carry defective endotoxin receptors) or in C57Bl/6 mice it is abrogated in CD44$^{-/-}$ mice. In all panels, mean values and standard errors from at least four data points are shown.

Figure 4.

Phosphorylation of Eta-1/Opn is necessary for engagement of integrin receptors leading to IL-12 production but not for ligation of CD44 leading to IL-10 inhibition by macrophages.

A. Secretion of IL-12 was measured by ELISA (30) after culture of resident peritoneal macrophages with 6 nM of dephosphorylated natural Eta-1/Opn (dpEta-1), recombinant Eta-1/Opn (rEta-1) or recombinant phosphorylated Eta-1/Opn (rEta-1 ~ P) (33) for 6 h in defined medium at 37 °C. Dephosphorylated native Eta-1/Opn and recombinant (unphosphorylated) Eta-1/Opn do not induce IL-12 production but retain inhibitory activity for IL-10. Recombinant Eta-1/Opn phosphorylation with Golgi kinases (rEta-1 ~ P) confers IL-12 inducing activity while similar levels of phosphorylation by PKA and PKC do not restore this activity.

B. The phosphorylation status of Eta-1/Opn modifies its biological activity. Absence of phosphates in bacterial recombinent Eta-1/Opn (rEta-1) results in loss of IL-12 inducing activity, while phosphorylation of (native) Eta-1/Opn (n-Eta-1/Opn) conveys this function. In contrast, recombinant and native Eta-1/Opn equally inhibit IL-4-induced IL-10 secretion, while the peptide NK10 has no effect.

FIGURE 1

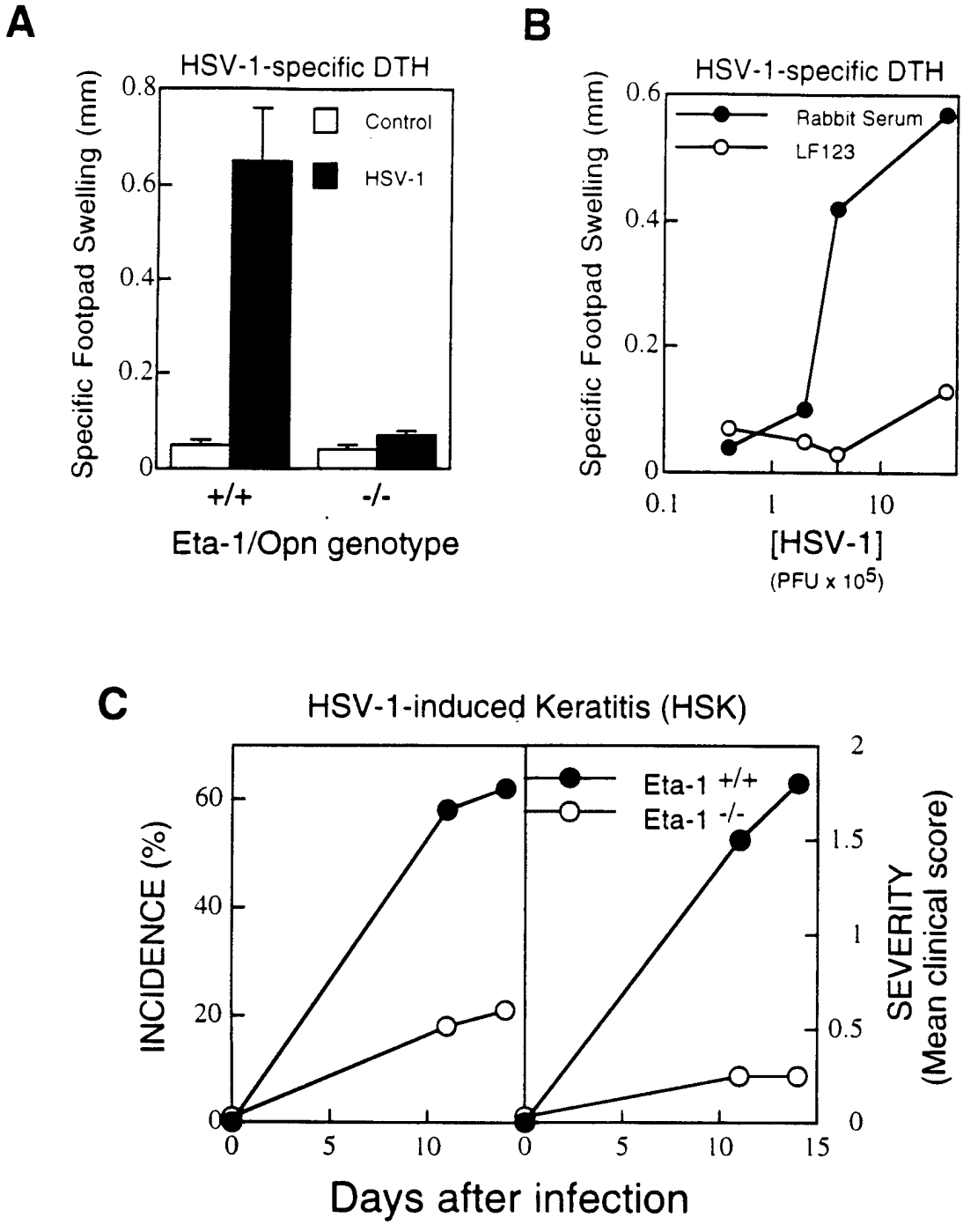
A
HSV-1-specific DTH
Specific Footpad Swelling (mm)
0.8
0.6
0.4
0.2
0
Control
HSV-1
+/+
-/-
Eta-1/Opn genotype
B
HSV-1-specific DTH
Specific Footpad Swelling (mm)
0.6
0.4
0.2
0
Rabbit Serum
LF123
0.1
1
10
[HSV-1]
(PFU x 10^5)
C
HSV-1-induced Keratitis (HSK)
INCIDENCE (%)
60
40
20
0
Eta-1 +/+
Eta-1 -/-
2
1.5
1
0.5
0
SEVERITY
(Mean clinical score)
0
5
10
0
5
10
15
Days after infection

FIGURE 1

D

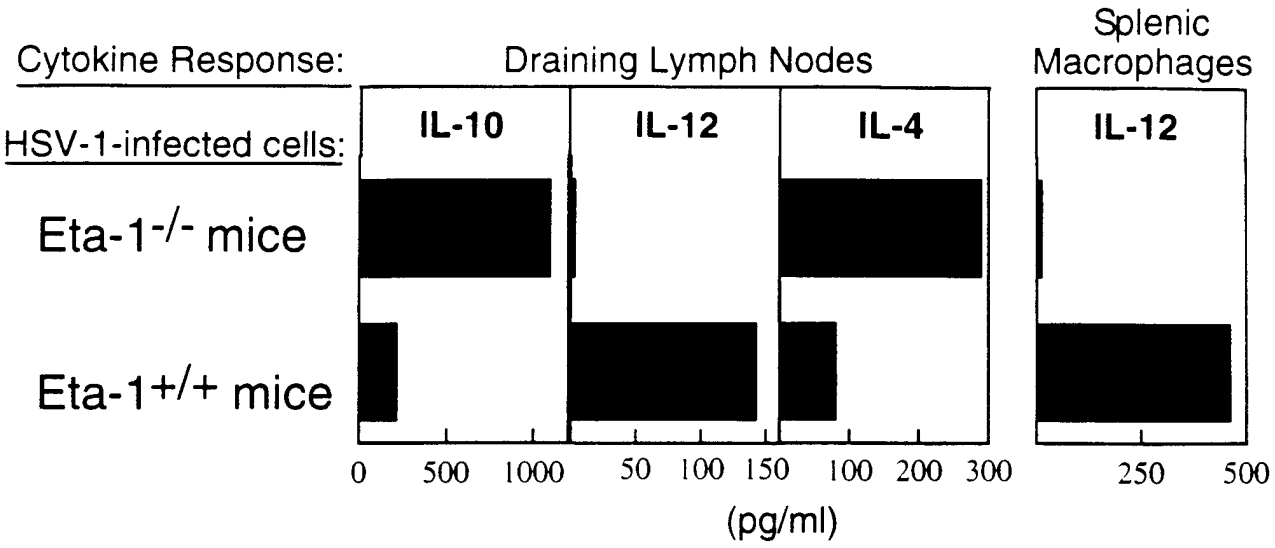
Cytokine Response:
Draining Lymph Nodes
Splenic Macrophages
HSV-1-infected cells:
IL-10
IL-12
IL-4
IL-12
Eta-1-/- mice
Eta-1+/+ mice
0
500
1000
50
100
150
100
200
300
250
500
(pg/ml)

FIGURE 2

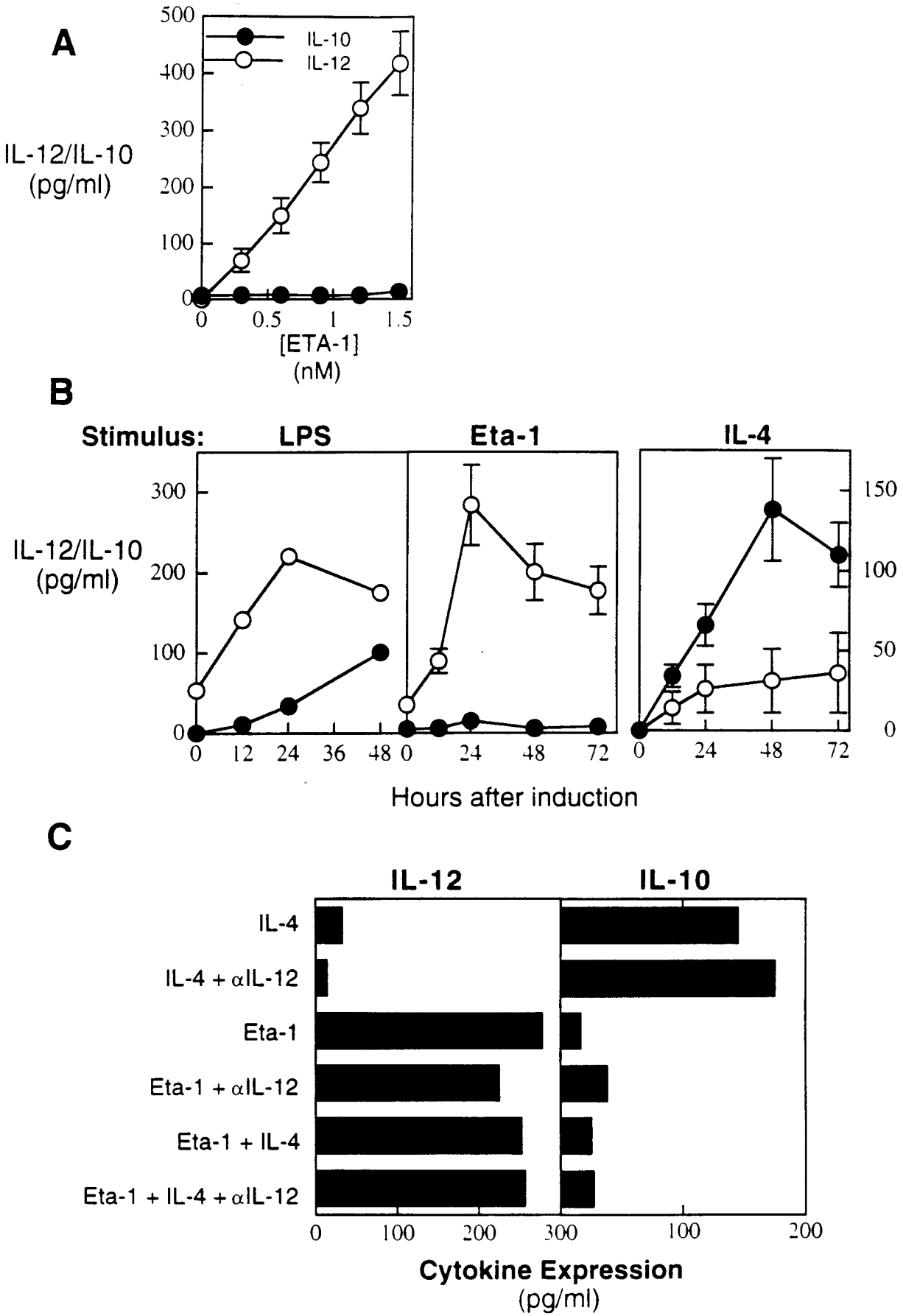
A
IL-12/IL-10
(pg/ml)
500
400
300
200
100
0
IL-10
IL-12
0
0.5
1
1.5
[ETA-1]
(nM)
B
Stimulus:
LPS
Eta-1
IL-4
IL-12/IL-10
(pg/ml)
300
200
100
0
150
100
50
0
0
12
24
36
48
0
24
48
72
0
24
48
72
Hours after induction
C
IL-12
IL-10
IL-4
IL-4 + αIL-12
Eta-1
Eta-1 + αIL-12
Eta-1 + IL-4
Eta-1 + IL-4 + αIL-12
0
100
200
300
100
200
Cytokine Expression
(pg/ml)

FIGURE 3

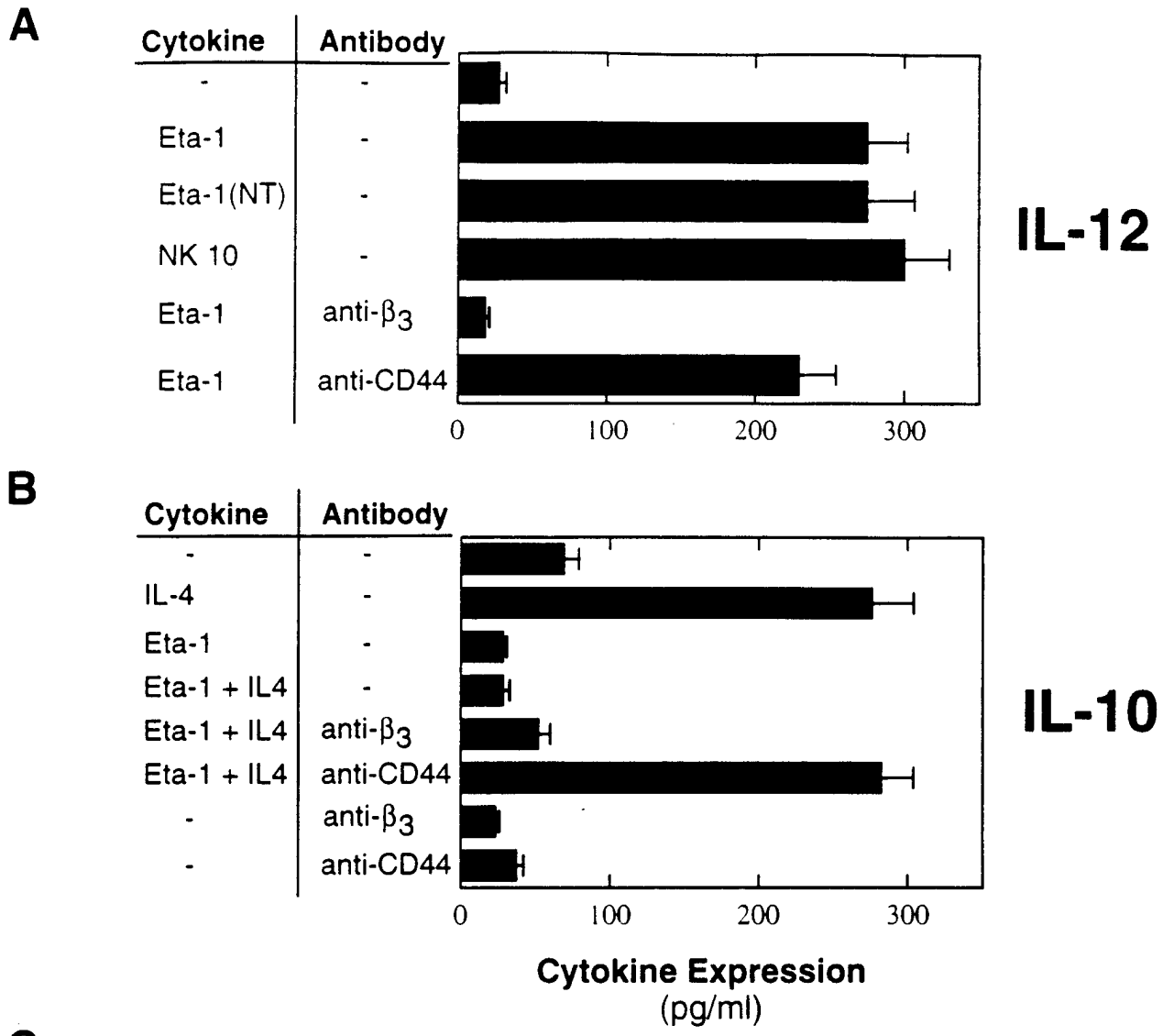
A
Cytokine
Antibody
-
-
Eta-1
-
Eta-1(NT)
-
NK 10
-
Eta-1
anti-β3
Eta-1
anti-CD44
0
100
200
300
IL-12
B
Cytokine
Antibody
-
-
IL-4
-
Eta-1
-
Eta-1 + IL4
-
Eta-1 + IL4
anti-β3
Eta-1 + IL4
anti-CD44
-
anti-β3
-
anti-CD44
0
100
200
300
IL-10
Cytokine Expression
(pg/ml)
C
Mouse Strain
IL-12
IL-10
C3H.HeJ
C57BL/6
(CD44 -/-)
C57BL/6
0
50
100
150
200
0
50
100
150
Cytokine Expression
(pg/ml)
Stimulus:
None
Eta-1
Stimulus:
IL-4
IL-4 + Eta-1

FIGURE 4

A

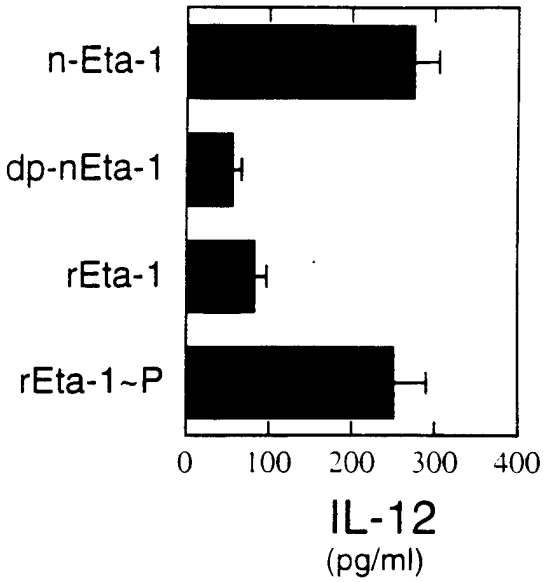
n-Eta-1
dp-nEta-1
rEta-1
rEta-1~P
0
100
200
300
400
IL-12
(pg/ml)

B

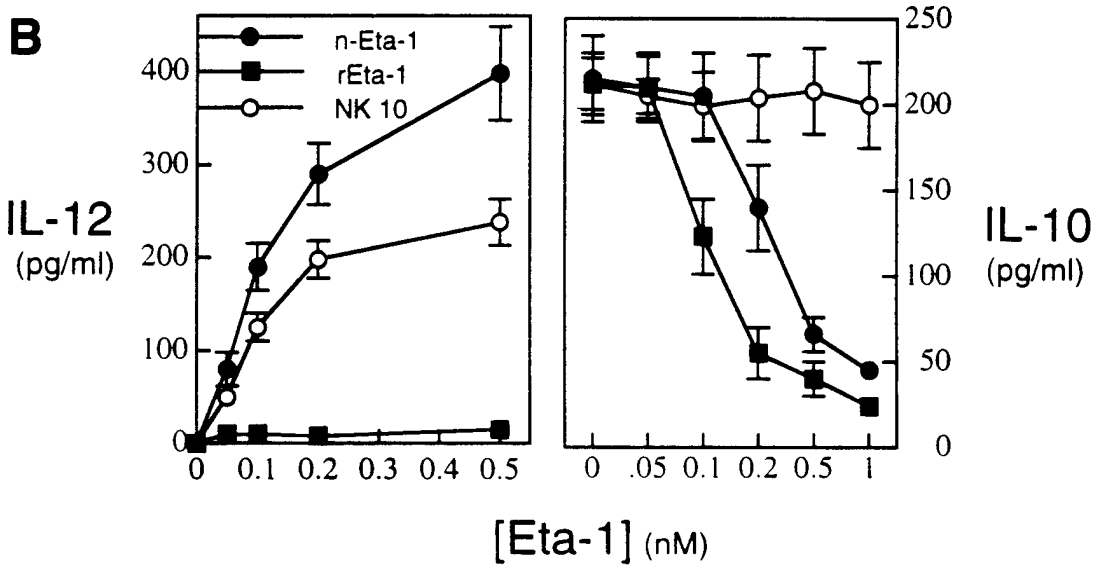
n-Eta-1
rEta-1
NK 10
IL-12
(pg/ml)
400
300
200
100
0
0 0.1 0.2 0.3 0.4 0.5
250
200
150
100
50
0
0 .05 0.1 0.2 0.5 1
IL-10
(pg/ml)
[Eta-1] (nM)

Phosphorylation-dependent Interaction of Osteopontin with its Receptors Regulates Macrophage Migration and Activation

Key terms: Osteopontin, phosphorylation, integrins, macrophages, delayed type hypersensitivity, T-cells, metalloproteases

Georg F. Weber[2,3*], Samer Zawaideh[1], Sherry Hikita, Vikram A. Kumar[2], [+]Harvey Cantor[2,4]. and Samy Ashkar[1*],

[1]Laboratory for Skeletal Disorders and Rehabilitation, Department of Orthopedic Surgery, Children's Hospital, Harvard Medical School, 300 Longwood Avenue, Boston, MA 02115

[2]Department of Cancer Immunology & AIDS, Dana-Farber Cancer Institute

Departments of Medicine[3] and Pathology[4], Harvard Medical School, 44 Binney Street, Boston, MA 02115

[*] These authors contributed equally to this project.

[+] Address correspondence to Samy Ashkar Childrens Hospital 300 longwood Ave. Boston MA. 02115 . Tel:617-355-7015; fax 355 713-4227; E mail Ashkar@A1.tch.harvard.edu

ABSTRACT

Secretion of the phosphoprotein osteopontin by activated T-cells confers resistance to infection by several intracellular pathogens through recruitment and activation of macrophages. Here we analyze the structural basis of this activity following cleavage of the phosphoprotein by thrombin into two fragments. We find that an interaction between the C-terminal domain of osteopontin with the CD44 receptor induces macrophage chemotaxis and inhibits cytokine secretion, while engagement of integrin receptors by a non-overlapping N-terminal osteopontin domain induces cell spreading, macrophage activation,cytokine secretion and phagocytosis. Serine phosphorylation of the osteopontin molecule is required for functional interaction of osteopontin and the N-terminal thrombin fragment with integrins. However, phosphorylation is not necessary for the interaction of the protein or its c-terminal thrombin fragment with CD44 receptors. Thus, in addition to regulation of intracellular enzymes and substrates, phosphorylation also regulates the biological activity of secreted cytokines. These data, taken as a whole, indicate that the activities of distinct osteopontin domains are required to coordinate macrophage migration and activation and dictates whether the immune reaction proceeds via a TH1 and TH2 response.

INTRODUCTION

The homing of macrophages to sites of infection or wound healing is an active process of translocation of cells across extracellular matrix barriers. Homing of macrophages into tissues requires local proteolysis of the extracellular matrix, pseudopodial extension, and cell mobility (30). Expression of this phenotype is not caused by one single gene or protein, but is a tightly control process involving the coordinated expression of multiple genes. This Physiological invasion is tightly regulated and ceases when the stimulus is removed (33; 36-39).

At the biochemical level, cell homing and physiological invasion appears to be similar in a number of physiological processess such as angiogenesis (33; 34), connective tissue remodeling, wound healing, immunological response, and nerve growth cone extension.

Invasion within a three-dimensional matrix requires the protrusion of a cylindrical pseudopod prior to the translocation of the whole cell body (40; 41). Several pieces of evidence point to pseudopodia, as the organs of motility and invasion. First, pseudopodial cell fragments lacking nuclei were shown to retain sensing and directional locomotive. Capacity (40; 41), proving that they have all the sensory and motor equipment necessary for crawling. Also, cell surface degradative enzymes and adhesion receptors appear to aggregate at pseudopodia (42). Furthermore, pseudopodia protrude at the point of surface stimulation by ligands which cause migration (40-42). The cytoskeleton is critical for pseudopodial extension. The internal actin structures provide the mechanical basis for pseudopodia, extension into free space at the area of binding of the ligands which induce migration (41; 43). The extension of pseudopodia is coupled with the other cellular events involved in invasion. A series of proteins on the surface of the

pseudopod coordinate sensing, protrusion, burrowing, and traction. The invading cell must mesh local proteolysis (38) with limited attachment and detachment (44). The leading edge of the cell must express activated proteinases. Then, as the cell moves into the zone of lysis, adhesion of the leading edge is required to grip the extracellular matrix and pull the cell forward and proteolysis must stop. The rear of the cell must detach from previous attachment sites to allow the cells to move forward. Further, pseudopod extension is essential for macrophage phagocytosis.

Macrophages play a critical role in wound healing and the efficient development of inflammatory responses. Protection against most infectious pathogens depends, in part, on secretion of T-cell cytokines that attract monocytes to sites of infection and activate these emigrant cells to express bacteriocidal activity {99}. An important component of this T-cell response is osteopontin, which mediates macrophage chemotaxis *in vitro* {577}, recruits monocytes to inflammatory sites *in vivo* {108} and regulates immunological resistance to several intracellular pathogens {99,100}. For example, inbred mouse strains that carry an allele of osteopontin, which allows high level expression in activated T-cells, are resistant to lethal effects of infection by the intracellular bacterial parasite *Rickettsia tsutsugamushi.* In contrast, inbred strains carrying a low expression allele do not develop a population of bacteriocidal monocytic migrants at the area of infection and succumb to systemic bacteremia {127}. Osteopontin expression has also been linked to granuloma formation, where it may regulate the chronic cellular response associated with tuberculosis infection and silicosis {1027}. Osteopontin has also been linked to efficient wound healing. Osteopontin null mice fail to heal properly (Liaw et al., 1998)

Osteopontin has been implicated in both cell attachment {487,545,546} and cell motility {542,577}. The protein contains sites which, bind to calcium, apatite, and heparin {552} and may be secreted in phosphorylated {896,897,898} and nonphosphorylated forms {787,543,889,890}.

Phosphorylation is functionally important because it may determine whether osteopontin associates with the cell surface or with the extracellular matrix {668,663}. Other posttranslational modifications, including sialylation, may also contribute to receptor ligation on certain cells {902}.

The osteopontin ligand binds to two classes of receptors. Engagement of the homing receptor CD44 through a non-RGD cell binding domain of osteopontin is sufficient to induce chemotaxis or attachment {551,577}. Binding of osteopontin to $\alpha_v\beta_3$ integrin receptors via its Gly-Arg-Gly-Asp-Ser (GRGDS) motif {108,546,542} may contribute to osteoclast adherence and resorption of bone {552} as well as to haptotaxis of endothelial cells {891,585}, vascular smooth muscle cells {540}, myelomonocytic cells {893}, and tumor cells {899}. Vascular smooth muscle cells may also engage osteopontin through $\alpha_v\beta_1$ and $\alpha_v\beta_5$ integrins in an interaction that leads to adhesion of cells but not migration {542}, and adhesion to immobilized osteopontin via integrins α_4 and α_5 has been reported {893}. Further Sanger et al., have demonstrated that endothelial cells attach better to thrombin cleaved OPN, suggesting, again, a physiological role for OPN cleavage during wound healing and inflammatory response.

The structural basis for the interaction of osteopontin with macrophages leading to migration and perhaps activation is incompletely understood. Here we show that engagement of β_3-integrin and CD44 receptors by separate domains of osteopontin leads to the expression of two distinct macrophage response phenotypes and that the interaction of integrin receptors with osteopontin is regulated by phosphorylation of the ligand.

MATERIALS AND METHODS

Cell lines. A31 is an integrin $\alpha_v\beta_3^-$, CD44$^-$ murine embryonic fibroblast clone derived from Balb 3T3 cells (CCL-163, ATCC). A31 cells transfected with CD44 (A31.C1) or A31 mock-transfectants were generated as described {577}. P388D1 is a transformed myelomonocytic lymphoma cell line derived from a DBA/2 mouse (CCL-46, ATCC). MH-S is a macrophage cell line that was derived by SV40 transformation from an adherent cell enriched population of alveolar macrophages (CRL-2019, ATCC) this cell line expresses CD44s, CD44(v6-v10), Mac-1, integrin $\alpha_v\beta_3$, and integrin subunits β_1, β_5. MT-2/1 is a thymus-derived macrophage from a Balb/c mouse that was immortalized by infection with retroviral vector {709}. It expresses CD44 and integrin $\alpha_v\beta_3$.

Osteopontin purification and cleavage. Recombinant GST-osteopontin fusion protein was derived from E. coli, digested with factor Xa and purified by affinity chromatography, as described {804,539}. Osteopontin was purified to homogeneity as determined by N-terminal sequencing. The native osteopontin used in this study is a full-length protein that is O-glycosylated and highly sialylated, free of sulfate or N-glycosylation and contains 15-17 phosphate residues. Thrombin cleavage and phosphorylation of osteopontin was accomplished by human thrombin (Sigma Chemicals), Golgi kinases or casein kinase II as described {804,539,549}.

Purification of osteopontin: Osteopontin was purified from conditioned media of MC3T3.C6, a cell clone derived from MC3T3E1 osteoblast like cell line that was selected for over production of OPN. Briefly, MC3T3.C6 was grown in defined media consisting of DME/H12 supplemented with pyruvate, insulin, transferrin, selenium and ethanol amine in a humidified atmosphere of 5% CO2 at 37oC.. Conditioned media from confluent cultures were collected

every 24 h. and stored frozen until processed. 1 liter of conditioned media was concentrated, into PBS, to 100 ml using Millipore tangential flow system (membrane cut off of 10,000daltons). The concentrated protein solution was applied to Millipore LC100 equipped with a DEAE-Memsep 1000 cartridge. The cartridge was developed with a discontinuous gradient of 0 to 1 M NaCl in phosphate buffer, pH 7.4. The major Osteopontin peak eluted at 0.26 M salt.

Osteopontin containing fractions were pooled concentrated by ultrafiltration (filtron 10,000 cut off) and applied to a chromatofocusing mono P column (pharmacia) at pH 8.2. After washing, the column was developed with polybuffer 74 (pharmacia). The major Osteopontin containing fractions eluted from the monobeads at pH 4.6. The protein was judged pure by several criteria including , SDS electrophoresis, and amino acid sequence analysis (N-terminal and internal peptide analysis). Mass spectroscopic analysis revealed a broad peak centered around a mass of 35,400 as expected from a highly modified protein. The protein was highly phosphorylated (11 mols of phosphate/mol of protein) was O-glycosilated but not N-glycosylated. and did not contain any measurable sulfate.

Dephosphorylation of OPN. 5 mg of OPN was dephosphorylated using 6 units (60 units/mg) type II potato acid phosphatase (Sigma # p3752) by a modification of a previously published procedure. Briefly, 5 mg of OPN were incubated with 6 U of acid phosphatase in 20 mM phosphate buffer pH 4.8 and incubated at 37°C for 2 h. After adjusting the pH to 8.2, the dephosphorylated protein was applied to a chromatofocusing column. The protein was eluted with polybuffer as described. Multiple peaks containing OPN were detected. The major peak eluted with a pH of 5.1. Amino acid analysis of the protein revealed a phosphate content of less than 1mol/mol protein.

Phosphorylation of rOPN: 5 mg of GST-OPN was phosphorylated as previously described. Briefly, rOPN was incubated at 37°C with 10 ug of golgi kinases in phosphate buffer containing 10mM ATP, 10 mM $MgCl_2$, 1mM $MnCl_2$,0.1 mM $CaCl_2$, 1uM cGMP, 1 mM pyrophosphate, 1 mM diacylglycerol, and 1 mM NaF. After 2 h, the phosphorylated protein was applied to a GSH-Sepharose column. The resin was washed with 5 volumes of PBS. The rOPN was eluted from the GSH-Beads by incubating the beads with 100U of factor Xa as described. After 2 h at 37°C, The released rOPN was applied to a chromatofocusing column. The phosphorylated rOPN was eluted from the resin with polybuffer 74 as described. The major peak eluted with pH 4.6. Phopho-amino acid analysis of the recovered protein revealed a phosphoserine content of 16 mol of phosphate/mol protein and 0.8 mols of phosphotherione/mol protein.

Spontaneous cell migration. Chemokinetic motility was assessed by a modification of the phagokinetic track assay {667}. Briefly, the surfaces of multi-well dishes were evenly coated with 0.99 μm diameter polystyrene beads (Polysciences, Warrington, PA). For testing the effect of osteopontin and its various modified forms on cell mobility, the beads were precoated with 5 μg/ml protein at 4°C overnight. Cells were layered on top of the beads at a density of 1000 cells/cm^2, incubated at 37°C in a humidified atmosphere of 95% air 5% CO_2 and the cultures were observed for

48 h after plating. The numbers of tracks formed by migrating cells were counted in photographs of random non-overlapping fields using phase contrast optics and analyzed for statistically significant differences.

Since cell adhesion is a prerequisite for chemotaxis, haptotaxis and cell spreading, Preliminary analysis of the adhesion of macrophages to OPN were conducted to evaluate the types of adhesion that can be mediated by the interaction of OPN to Macrophages. Two types of cell adhesion has been reported in the literature. Passive and active adhesion. Active adhesion of cells to substratum in pH and temperature dependent, is reduced by trypsin treatment and is dependent on the viability of the cell. Passive adhesion is temperature and pH independent, unaffected by trypsin treatment and is independent of cell viability and can mediate attachment to BSA, a protein generally considered a non-adhesive protein. To assure that the results of the interaction of OPN with macrophages are due to active attachment, preliminary experiments were conducted to examine passive vs active attachment of macrophages to OPN. Our preliminary analysis indicated that optimum results can be achieved if cells were harvested by non-enzymatic digestion from subconfluent cultures and limited exposure of the macrophages to temperature fluctuations. The viability of the cells was measured before and after the termination of the experiments and only data from experiments with greater than 95% cell viability were used. Further, under the conditions used in these experiments, cell attachment was temperature dependent, inhibitable by trypsin treatment and not affected by inhibitors of protein synthesis or secretion. Non passive attachment was less than 10%. In all our studies we have differentiated between attachment, adhesion and spreading. Attachment is mostly passive, is not associated with rearrangement of the cytoskeleton. Attached but not adhered cells cannot undergo G0-G1 transition (as judged by cyclin D expression), do not proliferate and become

non- viable within 6-12 hours. While attached cells can do rearrange their cytoskeleton, can undergo G0-G1 transition and can proliferate. Spread cells are arrested cells in G2 do not proliferate and are characterized by focal adhesion plaques. Most dye binding assays cannot differentiate between the three different types of attachment. In some of the dye binding assays one cannot differentiate between dead, cell debris or live cells. This is specially true for dyes like crystal violet that binds very tightly to dead cells.

Chemotaxis. Directed migration of cells was determined in multi-well chemotaxis chambers as described {564,577}. Briefly, two-well culture plates (Transwell) with polycarbonate filters (pore size 8-12 μm) separating top and bottom wells were coated with 5 μg fibronectin. 2 X 10^5 cells were added to the upper chamber and incubated at 37° C in the presence or absence of osteopontin in the lower chamber. After 4 h, the filters were removed, fixed in methanol, stained with hematoxylin and eosin and cells that had migrated to various areas of the lower surface were counted microscopically. Controls for chemokinesis included 200 ng of the appropriate form of osteopontin in the top well. All assays were done in triplicates and are reported as mean ± standard deviation.

Haptotaxis. Haptotaxis of MH-S or MT-2 monocytic cell lines to osteopontin or fragments of osteopontin was assayed using a Boyden chamber. The lower surface or both sides of polycarbonate filters with 8 μm pore size were coated with 5 μg of osteopontin. This concentration is saturating since osteopontin bound to filters with an EC_{50} of around 3.2 pM. 2 X 10^5 cells were added to the upper chamber, and incubated at 37° C in the absence of any factors in the lower chamber. After 4 h, the filters were removed, fixed in methanol and stained with hematoxylin and eosin. Cells that had migrated to the lower surface were counted under a microscope. All assays were done in triplicates and are reported as mean ± standard deviation.

***in vivo* cell migration.** Female C57BL/6 mice, purchased from Jackson Laboratories and housed at

the Redstone Animal Facility of the Dana-Farber Cancer Institute, were injected intraperitoneally with 200 μl of PBS containing varying dosages of K7 osteosarcoma-derived osteopontin. Injections of vehicle alone (PBS) served as negative controls. Mice were sacrificed by CO_2-asphyxiation at varying times after injection followed by immediate collection of peritoneal exudate by intraperitoneal injection and recovery of twice 10 mL PBS. Red blood cells were removed by hypotonic lysis with ACK buffer (0.15 M NH_4Cl, 1.0 mM $KHCO_3$, 0.1 mM Na_2EDTA, pH 7.4) for 5 minutes at room temperature. Cells were washed and resuspended in DMEM, 5% FBS for fluorescent antibody staining at a concentration of 0.2 to 1 million cells in 50 μl. Fluorescence-labeled antibodies (1 μg/1x10^6 cells) were incubated with cells for 30 minutes at 4°C, before washing twice with 200 μl of PBS and fixation in 500 μl of 2% paraformaldehyde in PBS. Analysis for cellular expression of CD44 (PE) together with CD11b (Mac-1, FITC, macrophage marker), B220 (FITC, B-cell marker), or CD3 (FITC, T-cell marker) was performed by dual-color flow cytometry with antibodies from PharMingen using a Coulter EPICS flow cytometer. Appropriate non-specific antibody controls and single color controls were included.

Cell spreading. Twenty-four well plates were coated with 10 μg/ml protein in PBS overnight at 4°C. Non-specific sites were blocked with 10 mg/ml BSA in PBS for 60 minutes. To preserve the integrity of adhesion receptors proliferating MH-S cells were collected using non-enzymatic cell dissociation solution (Sigma BioSciences) before resuspension in sterile Ca^{2+} and Mg^{2+}-free PBS and addition of 5x10^3 cells to each well and incubation at 37°C in 95% O_2/5% CO_2 for 1 hour. After removal of medium and loosely attached cells with sterile PBS, adherent cells were fixed with 1% paraformaldehyde, 1% glutaraldehyde in 0.1 M cacodylate buffer (pH 7.4) at room temperature for 1 hour, followed by staining with Hematoxylin solution for 1 hour, washing with distilled deionized water and staining with 0.1% Toluidine Blue overnight. Photomicrographs of 4-5 non-overlapping

fields were taken at 100X magnification for cell counting (Olympus microscope). Cell spreading was determined by membrane contour analysis and was scored according to increase in cell volume/surface area. In some experiments, cell spreading was also assessed by the formation of stress fibers. Each experiment was performed in quadruplicate wells and repeated 3 times.

Analysis of Signal Transduction. Signal transduction mechanisms were initially examined through the use of specific chemical inhibitors at the following final concentrations: 50 mM for cycloheximide, PKA inhibitors H89 at 1mM and, H7 at 20 uM, Inhibitors of PI pathway Wortmannin at 10 nM, Tyrosine kinase inhibitors genistein at 25 uM, PKC inhibitor chelerythrine at 20 uM, Casein Kinase II inhibitor quercetin at 6 mM . In all experiments using these compounds 2 x 10^6 macrophages were preincubated for 0.5 hours with the inhibitors before start of the experiment. Cell viability was determined by trypan blue exclusion on cell samples before and after the termination of the experiments. Cell viability in all reported experiments was > 95%. Microfilament disruption was carried out by preincubation of the cell cultures for one hour in 50 uM cytochalasin D. Microtubule dissociation was carried out by pre incubation of the cultures for 6 hours in 1 uM colchicine. All compounds were suspended in either DMSO or absolute ethanol and were added to the culture media at 1:1000 dilution. Controls were carried out with the corresponding vehicle. In separate experiments in which PKC and PKA were chemically activated 50 ng/ml phorbol 12-myristate 13-acetate and 10^{-5} M of forskolin were used respectively. In these experiments treatments were for 2 hours.

Immuno precipitation of PI-3 Kinase: Macrophages were lysed in 1 ml buffer A (10 mM Tris-HCl buffer, pH 7.2, containing 300 mM sucrose, 100 mM KCl, 1% Triton X 100 5 mM $MgCl_2$, 10mM EGTA, 0.1 mM sodium orthovanadate, 0.1 M e-amino-n-caproic acid, 5 mM benzamidine, 1 mM p-hydroxymercuribenzoate, 5 mg/l pepstatin, 1 mg/l leupeptin) at 4°C. After 10 min,

fractions containing 2 mg protein were pre-cleared by incubation with 100 μl of protein A insoluble at 4° C for 1 h. After centrifugation at 5000x for 10 min., the resultant supernatant was incubated with 0.1 mg of Rabbit polyclonal antibody raised against the p85a subunit of PI-3-Kinase (Upstate Biotechnology, Lake Placid, N.Y.). The immune complexes were collected by incubation with 10 l protein A-insoluble for 1 h at 4°C followed by centrifugation at 5000x for 10 min. The protein A-immuno complexes were washed 5x with lysis buffer, then once with 20 mM Tris-HCl. The immune complexes were released from the protein A beads by boiling the beads in 20 ml of SDS sample buffer containing 0.1% fresh 2-mercaptoethanol. The samples were resolved by on an 8% SDS-polyacrylamide gel (Laemmli, 1980), then transferred onto ECL-membrane by semi-dry blotting as described by the manufacturer. Phosphorylation of PI-3-Kinase was assessed by probing the membranes with anti-phosphotyrosine.

Zymography Secretion of proteinases was assayed by SDS-substrate gel electrophoresis under non-reducing conditions as described {913}. Briefly, cell culture supernatant was collected after 6 hours of culture, concentrated 5 times and resuspended in 200 μl zymogram buffer (40 mM Tris-HCl, pH 7.5) before addition to Laemmli sample buffer and electrophoresis in 10% polyacrylamide gels impregnated with 1 mg/ml gelatin. Following electrophoresis, gels were incubated for 30 min at 37°C in 50 ml of 50 mM Tris-HCl buffer, pH 8.0, containing 2% Triton-X100 and 10 mM $CaCl_2$ to remove the SDS, followed by incubation for 18 h in 50 mM Tris-HCl buffer, pH 8.0, containing 5 mM $CaCl_2$. After staining the gels with Coomassie Brilliant Blue, gelatin and casein degrading enzymes were identified as clear bands against a dark blue background.

RESULTS

Osteopontin interacts with CD44$^+$ and CD44$^-$ macrophages *in vivo*

Singh et al. {108} have reported an RGD-dependent interaction between osteopontin and integrin receptors and *in vivo* attraction of macrophages by subcutaneously injected osteopontin. We analyzed osteopontin-attracted macrophage populations for expression of CD44. Titration of soluble osteopontin into the peritoneum resulted in a dose dependent increase in the cellular infiltrate with a peak response occurring at 4-6 hrs at about 10 μg of osteopontin **(Figure 1A,B)**; the decreased response after 6 hours may reflect clearance of soluble osteopontin from the peritoneal cavity. The numbers of Mac-1$^+$ cells in the infiltrate were increased five-fold over basal levels and about 90% of peritoneal macrophages were CD44$^+$. Osteopontin injections induced a disproportionately high increase in both Mac-1$^+$CD44$^+$ as well as Mac-1$^+$CD44$^-$ cells, implying that ligation of both classes of osteopontin receptors may contribute to migration *in vivo*. The predominant migration of Mac-1$^+$ cells (about 65% of the infiltrate) is consistent with previous studies of osteopontin {108}, and is in contrast to the inflammatory response to lipopolysaccharide, which consists of roughly equal numbers of CD3$^+$, B220$^+$, and Mac-1$^+$ cells (data not shown). This cellular infiltratation is unlikely to reflect contamination of osteopontin, which was pure according to peptide sequence analysis, since co-injection of osteopontin with anti-osteopontin antibody prevented the influx of cells whereas rabbit immunoglobulin had no effect (data not shown).

Our previous investigations of stable transfectants of A31 cells indicated that the interaction of osteopontin with CD44 depended on expression of CD44 splice variants 3-6 {577}, which characterize activated lymphocytes {534}. More recent studies indicate that A31 cells which express the standard form of CD44 (lacking variant exons) do not bind osteopontin (data not shown). These findings are consistent with the finding that lymphocytes attracted into the peritoneal

cavity appear to be activated as judged by increased forward scatter measurements in flow cytometry (Figure 1A,B).

Earlier studies of osteopontin binding to the myelomonocytic cell line Wehi 3 suggested that this interaction depended mainly on engagement of integrin receptors {108}, while later investigations identified CD44 as a second receptor that was associated with chemotaxis {577}. To determine whether distinct domains of osteopontin were responsible for engagement of the two receptors, we exploited the observation that thrombin cleaves osteopontin into two fragments, an N-terminal 1-153 fragment containing the RGD motif and a 154-294 C-terminal fragment {666,539}.

The N-terminal domain of osteopontin induces spreading and activation of macrophages via integrin $\alpha_v\beta_3$

Macrophage spreading on extracellular matrix proteins depends, in part, on engagement of their integrin receptors. Spreading of the MH-S macrophage cell line on immobilized native osteopontin is mediated by the RGD-containing N-terminal thrombin cleavage fragment but not by the C-terminal fragment and is reversed by addition of soluble GRGDS but not control GRGES peptide. Moreover, phosphorylation of recombinant osteopontin is required for this activity **(Figure 2).**

We assessed the contribution of interactions between immobilized osteopontin and integrin receptors to cell motility. Beads coated with native phosphorylated osteopontin or recombinant osteopontin that had been phosphorylated by Golgi-kinases or casein kinase II, but not unphosphorylated recombinant osteopontin or recombinant osteopontin phosphorylated with protein kinase A, C, or G, completely inhibited random migration by the myelomonocytic cell line P388D1 **(Figure 3)**, suggesting that P388D1 cells recognize and are affected by a specific form of

immobilized phosphorylated osteopontin. We then investigated the ability of the immobilized ligand to induce monocyte haptotaxis, as judged by cell migration through poly-carbonate filters. Osteopontin induced monocyte migration that was mainly directional (i.e., the cells responded to a positive gradient of bound osteopontin), and thus haptotactic and was inhibited by GRGDS and antibody to β_3 chain of integrins but not by antibody to CD44 **(Table I)**.

Because cell spreading and haptotaxis is often associated with cellular activation, we asked whether the interaction between phosphorylated osteopontin and macrophages leads to signs of activation according to secretion of metalloproteinases. Adhesion of macrophage to the phosphorylated N-terminal fragment but not the C-terminal fragment of osteopontin induced strong MMP-2 (gelatinase A) and MMP-9 (gelatinase B) activity and induction was inhibited by GRGDS but not GRGES **(Figure 4)**.

The C-terminal domain of osteopontin interacts with CD44 to induce chemotaxis

Stable CD44 transfectants of $\alpha_v\beta_3$ fibroblasts which do not express integrin {577} were used to examine the interaction of CD44 with osteopontin. The C-terminal but not the N-terminal cleavage fragment mediated chemotaxis of A31.C1/CD44 stably transfected cells **(Table 2A)**, but not mock-transfected A31.MLV cells, confirming the dependence of cell migration on the expression of CD44. The C-terminal fragment also induced chemotaxis of macrophage cell line MH-S as efficiently as intact osteopontin, while the N-terminal 30 kDa osteopontin fragment was inactive **(Table 2B)**; equimolar mixtures of both fragments displayed activity similar to that of the 28 kDa C-terminal fragment alone (data not shown). These results, taken together, indicate that the chemotactic domain of osteopontin resides in the 28 kDa C-terminal part of the molecule.

DISCUSSION

The central result of the present structure-function analysis of osteopontin is that engagement of its two receptors by distinct domains of osteopontin leads to different monocyte responses. The binding site for CD44 resides within the C-terminal region of osteopontin and mediates chemoattractant activity. In contrast, the RGD motif within a non-overlapping N-terminal portion of osteopontin, exposed after phosphorylation or thrombin cleavage, can mediate haptotaxis and cellular activation. In addition, the domains also exert specific changes in signal transduction enzymes and gene expression. Thus, in addition to the well-established role of phosphorylation in regulating the biological interactions of intracellular enzymes and their substrates, phosphorylation of a secreted extracellular protein also can provide molecular information that targets a protein to particular interaction partners which dictate its biological activity.

The participation of monocytes/macrophages in inflammation entails emigration of these cells from peripheral blood into infected tissues, where they produce cytokines that regulate diverse processes including anti-microbial activity, cell growth, differentiation and wound healing {1024}. Emigration of monocytes depends on coordinate engagement of different subsets of cell surface receptors by cytokines and extracellular matrix that underlie migration and/or adhesion within various anatomic compartments. Macrophages participate in two general types of inflammatory reactions. In immediate inflammatory responses, macrophages are attracted and activated by neutrophils and support a reaction that usually is characterized by excessive fibrotic response and scar formation. In contrast, delayed type hypersensitivity responses include inflammation associated with resistance to infection by intracellular pathogens and enhancement of wound healing.

Differential expression of osteopontin by T-cells determines the relative levels of these two

responses. Resistance to *Rickettsial* infection, mediated by vigorous induction of osteopontin, leads to an early monocyte influx into infected sites and rapid acquisition of macrophage bacteriocidal activity. Susceptibility of cells to *Rickettsial* infection, on the other hand, reflects delayed and weak osteopontin responses and is characterized by an early accumulation of neutrophils at sites of infection {99,592}. High levels of osteopontin expression are also a hallmark of monocytic granulomatous reactions in the context of tuberculosis and silicosis {1027} and may play a central role in the revascularization process that is essential for wound healing {1028}.

Proteolysis can also play an important role in regulating the type and intensity of inflammatory responses. Selective recruitment of neutrophils to sites of immediate inflammatory responses is enhanced by the release of the 7S domain of collagen type IV and entactin, while macrophages can be recruited in delayed-type hypersensitivity by fibronectin fragments {1023}. One consequence of macrophage activation by the N-terminal portion of osteopontin is secretion of metalloproteases. These constitute a family of at least 14 proteolytic enzymes that have distinct but overlapping substrate specificity. Metalloproteases 2 and 9 cleave type IV collagen and therefore may be essential for migration of monocytes through basement membranes {1026}. Metalloproteases may also release TNFα, EGF, and TGFα from cell membranes and allow these cytokines to activate monocytes and mesenchymal cells and stimulate angiogenesis {1025}.
The paradigm for activation of Ras and extracellular signal-regulated kinase (ERK)/mitogen-activated protein (MAP) kinase by extracellular stimuli via tyrosine kinases, Shc, Grb2, and Sos does not encompass an obvious role for phosphoinositide (PI) 3-kinase, and yet inhibitors of this lipid kinase family have been shown to block the ERK/MAP kinase signalling pathway under certain circumstances. Various studies have suggested a requirement of the lipid kinase phosphatidylinositol-3 kinase (PI3- kinase) in this process. PI3kinase regulates the activation status

of the small GTP-binding protein Rac which, in turn, is able to activate another G-protein Rho. Rac and Rho are known to regulate the structure of the membrane- and cytoplasmic actin-cytoskeleton. We have demonstrated that the regulation of cell shape in macrophages corrolates with changes in gene expression andcis mediated in parft through PI-3-Kinase. These results are consistant with previous results showing regulation of IL-10, IL-12, TNFa and TgFb with activation or deactivation of PI-3-Kinase.

Our findings suggest that attraction and activation of monocytes depends, in part, on orchestrated activities of osteopontin binding domains that have been modified by thrombin {666}, ecto-kinases {905} and ecto-phosphatases {663}. Thrombin cleavage of osteopontin that has been integrated into the matrix through transglutaminases {626} can lead to the release of chemotactic C-terminal osteopontin fragment and attraction of monocytes to a site of infection. Subsequent engagement of integrin receptors on emigrant monocytes by immobilized phosphorylated N-terminal domain of osteopontin may facilitate local haptotactic migration towards a site of microbial infection or inflammation. After arrival, attachment and spreading of emigrant monocytes mediated by engagement of $\alpha_v\beta_3$ integrin receptors by the N-terminal osteopontin thrombin cleavage product [possibly through increased access of the RGD binding site {891}], can lead to macrophage activation and expression of inflammatory mediators such as metalloproteases **(Figure 5)**. Although additional *in vivo* studies are required to test this model, definition of the functional domains of osteopontin in this report represents an important step in understanding this process and may allow the rational development of osteopontin analogs that antagonize or mimic discrete biological activities of the parent molecule.

ACKNOWLEDGEMENTS

This study was supported in part by National Institutes of Health research grant AI12184 to HC; National Institutes of Health grant CA76176 and Department of Defense breast cancer grant DAMD17-98-8060 to GFW; grants from MDPH, Army and a career development grant from Children's Hospital to SA; and National Institutes of Health grant AR34078 to MJG. SZ was supported by a grant from the Fullbright Foundation. The authors are grateful to Alison Angel and Lisa Lagasse for assistance in the preparation of the manuscript.

REFERENCES

33. Folkman I Tumor angiogenesis: therapeudic implications. N Engl J Med 1971; 285, 1182-1186.

34. Weidner N. Tumor angiogenesis: review of current applications in tumor prognostication. Semin Diagn Pathol 1993; 10, 302-313.

35. Talhouk RS, Bisell MJ, Werb Z. Coordinated expression of extracellular matrix degrading proteinases and their inhibitors regulates mammary epithelial function during involution. J Cell Biol 1992; 118, 1271-1282.

36. Wu DY, Goldberg DJ. Regulated tyrosine phosphorylation at the tips of growth cone filopodia. J Cell Biol 1993; 123, 653-664

37. Lola PK, Graham CH. Mechanisms of trophoblast invasiveness and their control: the role of the proteases and protease inhibitors. Cancer Metastasis Rev 1990; 9, 369-380.

38. Liotta LA, Steeg~ PS, Stetler-Stevenson WG. Cancer metastasis and angiogenesis; an imbalance of positive and negative regulation. Cell 1991; 64, 327-336.

44. Damsky CH and Werb Z. Signal transduction by integrin receptors for extracellular matrix: cooperative processing of extracellular information. Curr Opin Cell Biol 1992; 4, 772-781.

45. Matrisian LM. Metalloproteinases and their inhibitors in matrix remodeling. Trends Genet 1990; 6, 121-125.

LEGENDS TO TABLES & FIGURES

Table 1. Haptotactic activity of osteopontin and the N-terminal fragment of osteopontin. A) Migration of MH-S across polycarbonated filters in response to bound osteopontin. Coated filters were placed in a Boyden chamber with the coated side up (top row), or down (left column). Or to both sides (diagonal). Data are expressed as migratory index (cells migrating in response to osteopontin/cells migration in response to buffer). Values are expressed as mean $\pm$ SEM. B) Inhibition of migration by osteopontin fragments or modulators of receptor interaction. Monocyte migration was mainly directional (i.e., the cells responded to a positive gradient of bound osteopontin), and thus haptotactic. Values above and along the diagonal were also greater than the buffer control, but less than that below the diagonal, indicating that a minor component of monocyte migration to bound osteopontin was random.

Table 2. Chemotactic activity is mediated by the C-terminal peptide released after thrombin cleavage of osteopontin. A) Chemotactic activity of osteopontin fragments after thrombin degradation, separation and purification was tested in a modified Boyden chamber {577}. Purified natural osteopontin exerted chemotactic activity for $CD44^+$ A31.C1 cells. The C-terminal (CT) thrombin cleavage product (pos 154-294) but not the N-terminal (NT) thrombin cleavage product (pos 1-153) of osteopontin also mediated chemotaxis. B) as A) but the migration of MH-S monocyte cell line. C) Inhibition of migration by osteopontin fragments or modulators of receptor interaction.

Figure 1: Titration of osteopontin into the peritoneum induces a cellular infiltrate in a dose dependent manner. The numbers reflect A) ratios of total cells (O) or B) cells with the surface

markers Mac-1^+ (_), $B220^+$ (■) or $CD3^+$ (□) in mice injected with osteopontin versus mice injected with PBS (Cell numbers for PBS-injected mice ranged from: 443,000 to $1.1x10^6$ cells total; 224,000 to 596,000 Mac-1^+ cells; 31,300 to 176,000 $B220^+$ cells; 18,100 to 214,100 $CD3^+$ cells). Osteopontin may preferentially attract activated immune cells since lymphocytes attracted into the peritoneal cavity appear to be activated as judged by increased forward scatter measurements in flow cytometry.

Figure 2: Phosphorylation of osteopontin is required to induce cell spreading. MH-S monocytic cells (10^3/well) were incubated in 96-well plates that had been coated with 10 μg/ml of the indicated ligands for 1 hr and stained with toluene blue. A) (1) MH-S cells attached to immobilized phosphorylated osteopontin and (2) MH-S cell bound to unphosphorylated osteopontin. (Original magnification 400X) B) The numbers of cells that attached after 1h incubation in wells containing the indicated ligands are shown on the left and the proportion of these cells that were spread is shown on the right. The presence of soluble GRGDS (1 mM) is indicated by open bars.

Figure 3: Chemokinetic motility on plastic surfaces. Cell migration in dishes containing 0.99 μm diameter polystyrene beads that were not coated or coated with 5 μg/ml of protein at 4°C overnight. The number of migrating cells based on phase contrast tracking (top left: phagokinetic track on uncoated beads, top right: reduced track on beads coated with phosphorylated osteopontin) in cultures containing beads coated with the indicated material: No protein; Fibronectin; Natural osteopontin; Recombinant osteopontin; Recombinant osteopontin phosphorylated (P-osteopontin) with PKA; Recombinant osteopontin phosphorylated (P-Opn) by Golgi kinase; Opn-NT; and Opn-CT. Cell motility ($3x10^3$ cells/cm^2) was assessed over 48 h according to formation of phagokinetic

tracks {667}.

Figure 4: Induction of metalloprotease secretion by phosphorylated but not unphosphoryltated osteopontin. MH-S cells were stimulated for 6 hours with either phosphorylated or unphosphorylated osteopontin at a concentration of 10 μg/ml in serum-free defined medium. In order to visualize the secreted metalloproteases, gelatin zymograms were performed using a modification of Giunciuglio et al. {895} (see Materials and Methods). MMP-9 and MMP-2 are both visible in the sample stimulated with natural osteopontin (lane 1) and samples stimulated with phosphorylated r-Opn (lane 2). Control: MH-S cells were incubated with serum-free defined medium (lane 3). MMP9 but not MMP2 is stimulated by the N-terminal fragment of osteopontin (Opn) (lane 4), while the C-terminal fragment of osteopontin has little or no stimulatory activity (lane 5). Dephosphorylation of osteopontin with acid phosphatase abolishes the stimulatory activity of osteopontin (lane 6). Similarly, rOpn has no stimulatory activity (lane 7). The results demonstrate that only phosphorylated osteopontin had a stimulatory effect the gelatinolytic activity secreted by MH-S cells.

Figure 5: A) Regulation of Cytokine Expression by OPN B) Effect of signaling inhibitors on OPN mediated activity

Figure 6: Regulation of PI-3-kinase by OPN

Figure 7: Model of monocyte regulation by osteopontin. Osteopontin is secreted by activated T-cells. Thrombin cleavage releases the two receptor-binding domains which carry out distinct functions in the cascade of events leading to macrophage attraction and activation. The C-terminal piece exerts chemotactic activity that is phosphorylation independent, leading to attraction of

macrophages to the cleavage site and cellular attachment to the Osteopontin N-terminal fragment. Phosphorylation-dependent haptotaxis on cross-linked Opn-NT leads to macrophage spreading and activation, including release of metalloproteases which can degrade the matrix and stimulate additional rounds of migration/attachment/activation.

Figure 1: GEORG

Table 1A

	Phosphorylated		
	Haptotactic index	Chemotactic index	Spreading index
control	1 ±	1 ±	1 ± 0.3
OPN	9.8± 0.9	13.3 ±1.9	10 ± 2.1
OPN-NT	1.8 ± 0.7	0.9 ±	11 ± 1.6
OPN-CT	1.6 ± 0.5	9.6 ± 1.9	2 ± 0.7
NT10k	4.2 ± 1.1	1.1 ±	5 ± 2.4
r OPN (GK)	12.6± 2.1	10.4 ±1.6	11 ± 1.7
r OPN (CKII)	8. ± 1.8	10.3 ±1.6	12 ± 3.1
r OPN (CKI)	10.± 1.9	9.9 ±2.3	8 ± 2.6
r OPN (PKG)	0.8± 0.4	8.7 ±2.0	1.0 ± 0.1

Table 1b

	Dephosphorylated		
	Haptotactic index	Chemotactic index	Spreading index
control	1 ± 0.3	1 ±	1±
OPN	3.6 ±	11.4 ±	2 ±
OPN-NT	0.6 ± 0.2	0.9 ±	11 ±
OPN-CT	1.3 ± 0.6	9.6 ± 1.9	2 ±
NT10k	1.8 ± 0.9	1.1 ±	7 ±
r OPN	1.5 ± 0.1	10.5 ± 2.2	2.4 ± 0.3

Figure 6

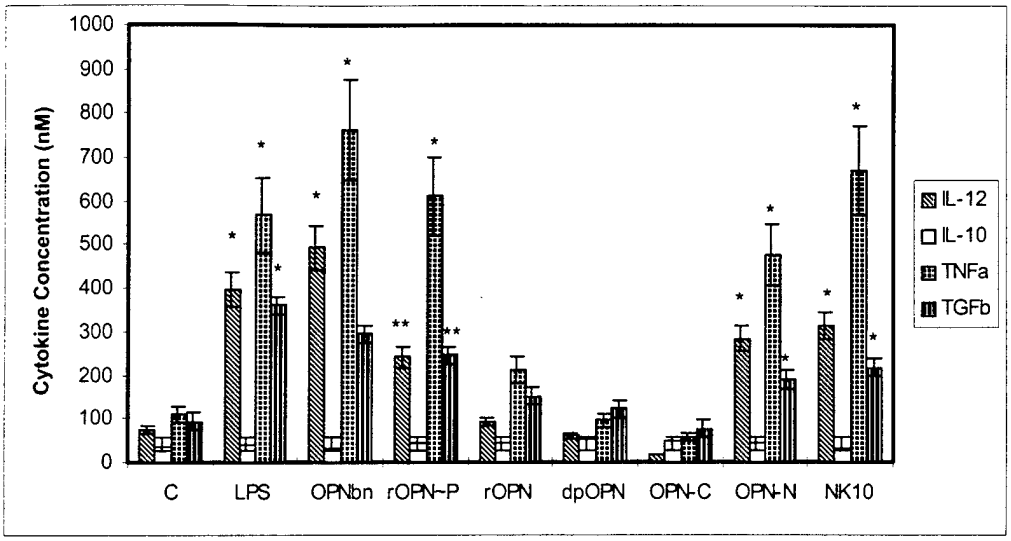
Cytokine Concentration (nM)
1000
900
800
700
600
500
400
300
200
100
0
C
LPS
OPNbn
rOPN-P
rOPN
dpOPN
OPN-C
OPN-N
NK10
IL-12
IL-10
TNFa
TGFb

TABLE 2 B

Inhibition of monocyte haptotaxis

	MI OPN	MI OPN-NT
control	9.8± 0.9	6.1 ± 0.7
+ GRGDS (1 mM)	**3.6 ± 1**	**2.1 ± 0.2**
+ anti CD44 (0.1 ug)	7.8 ± 0.7	5.5± 0.3
+ anti b3 (0.1 ug)	**4.8 ± 0.6**	**1.6 ± 0.1**
+ OPN-NT	**5.3 ± 0.8**	4.1± 0.3
+OPN-CT	7.3 ± 0.6	**5.2 ± 0.5**
+OPN	**5.1 ± 0.4**	**2.8 ± 0.4**

Table 2C

Inhibition of monocyte Chemotaxis		
	MI OPN	MI OPN-NT
control	13.3 ±1.9	11.9 ± 1.3
+ GRGDS (1 mM)	10.6 ± 1.3	12.7 ± 2.0
+ anti CD44 (0.1 ug)	7.8 ± 0.7	8.6 ± 0.9
+ anti β3 (0.1 ug)	9.8 ± 0.6	11.3 ± 2.1
+ OPN-NT	12.3 ± 2.0	10.0 ± 0.9
+OPN-CT	6.3 ± 0.7	3.7 ± 2.2
+OPN	4.4 ± 0.6	2.0 ± 0.7

Table 4 B
Inhibition of monocyte Chemotaxis

	MI OPN	MI OPN-CT
control	13.3 ±1.9	9.6 ± 1.9
+ GRGDS (1 mM)	10.6 ± 1.3	7.7 ± 1.6
+ anti CD44 (0.1 ug)	**7.8 ± 0.7**	**4.6 ± 0.7**
+ anti β3	10.6 ±1.5	12.1±2.1
+ PT	**3.8 ± 0.6**	**1.3 ± 2.1**
+ OPN-NT	12.3 ± 2.0	9.6 ± 1.9
+OPN-CT	**6.3 ± 0.7**	**3.7 ± 1.6**
+OPN	**4.4 ± 0.6**	**2.6 ± 0.2**

Inhibition of monocyte haptotaxis

	MI OPN	MI OPN-NT
control	**9.8± 0.9**	6.1 ± 0.7
+ GRGDS (1 mM)	**3.6 ± 1**	**2.1 ± 0.2**
+ anti CD44 (0.1 ug)	7.8 ± 0.7	5.5± 0.3
+ PT	8.8 ± 0.6	5.6 ± 0.1
+ OPN-NT	**5.3 ± 0.8**	4.1± 0.3
+OPN-CT	7.3 ± 0.6	5.2 ± 0.5
+OPN	**5.1 ± 0.4**	2.8 ± 0.4

TABLE 2A
HAPTOTACTIC RESPONSE OF MACROPHAGES TO OPN AND ITS DOMAINS

	OPN bound to upper side			
OPN bound to lower side	**0**	**1 ug**	**3 ug**	**5 ug**
0	**1.0 ± 0.15**	**1.5 ± 0.2**	**1.8 ± 0.1**	**0.6 ± 0.2**
1	**5.2 ± 0.35**	**1.5 ± 0.3**		
3	**7.8 ± 0.4**		**2.1 ± 0.3**	
5	**9.3 ± 0.8**			**2 ± 0.1**

TABLE 2 B

		LOWER CHAMBER			
		PBS	OPN	OPN CT (P174-343)	OPN NT (P1-173)
UPPER CHAMBER	PBS	56±10	3121±56*	478±98*	71±21
	OPN	34±7	168±24	305±50	36±19
	OPN CT	9±4	88±24	220±38	26±5
	OPN NT	63±11	287±60	409±55	14±5

Table 4 . Experiments were performed as described in tables 2 and3 Data are expressed as migratory index (cells migrating in response to OPN/cells migration in response to buffer). Bold numbers indicate p value less than 0.05

FIGURE 4 C

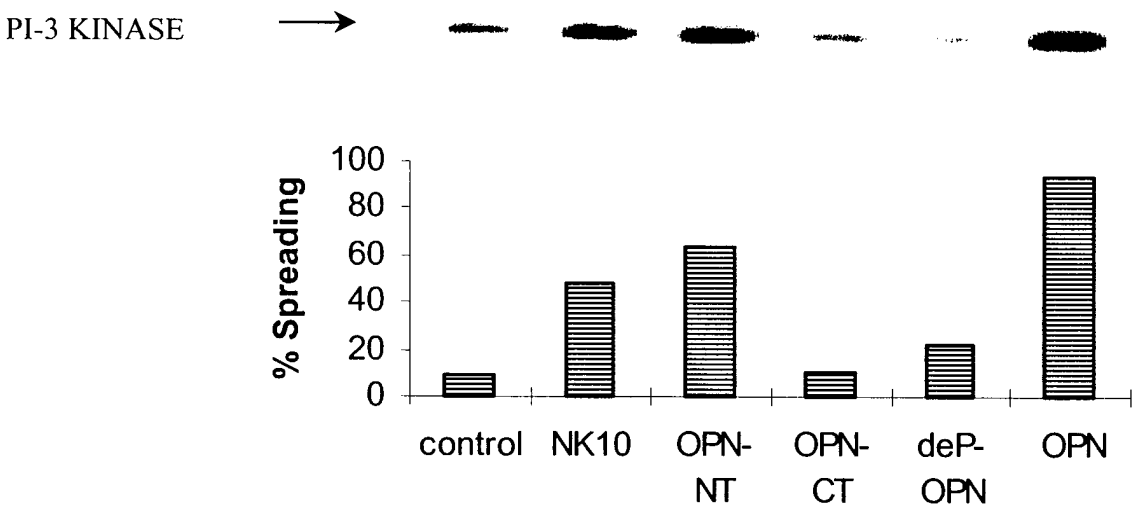
PI-3 KINASE
% Spreading
100
80
60
40
20
0
control
NK10
OPN-NT
OPN-CT
deP-OPN
OPN

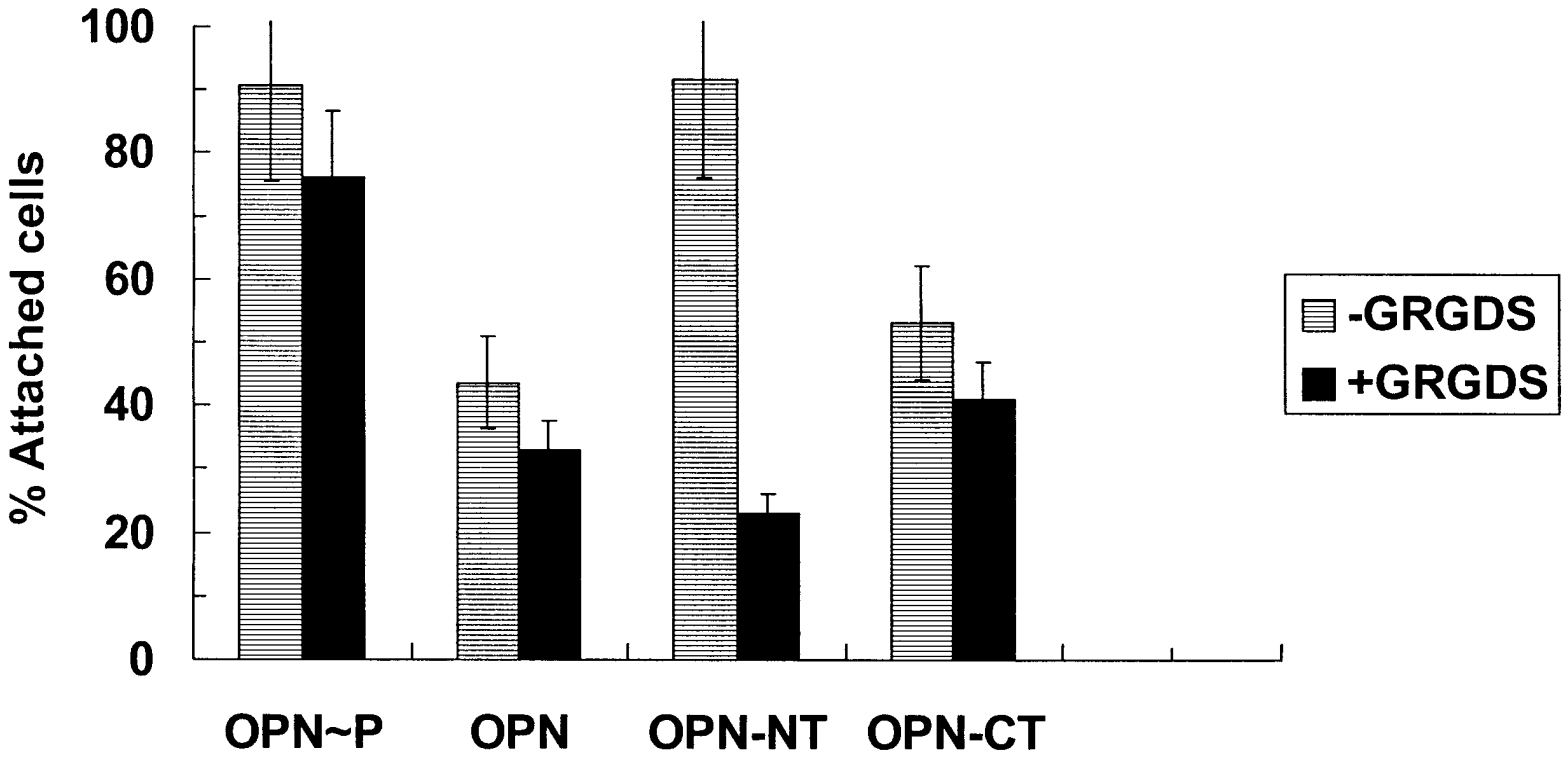
100
80
60
40
20
0
% Attached cells
OPN~P
OPN
OPN-NT
OPN-CT
-GRGDS
+GRGDS

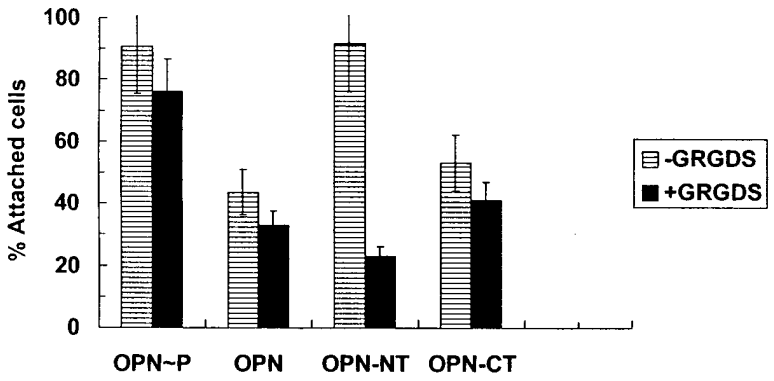
% Attached cells
100
80
60
40
20
0
OPN~P
OPN
OPN-NT
OPN-CT
-GRGDS
+GRGDS

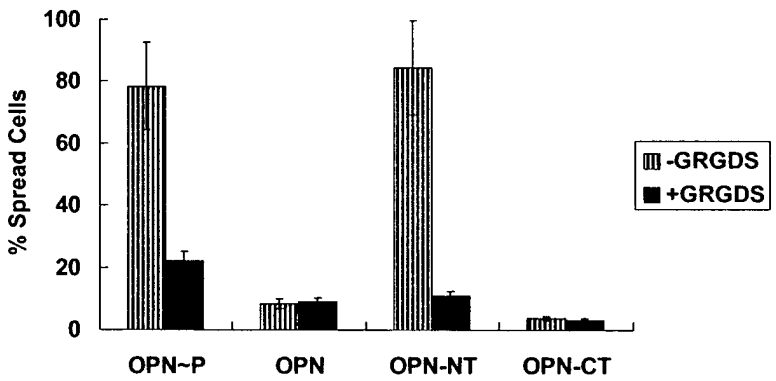
% Spread Cells
100
80
60
40
20
0
OPN~P
OPN
OPN-NT
OPN-CT
-GRGDS
+GRGDS

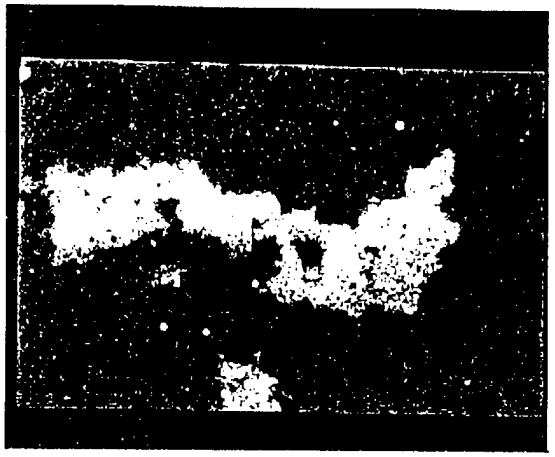

A

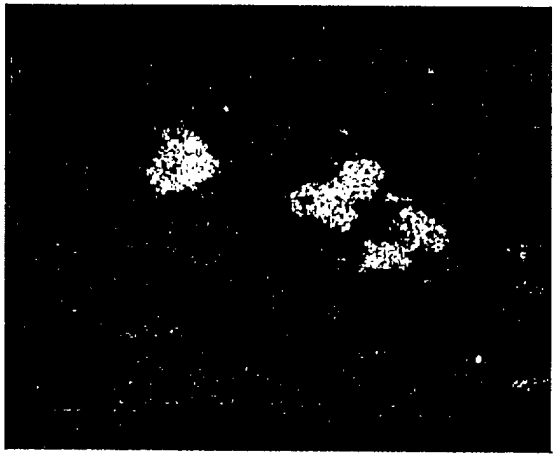

B

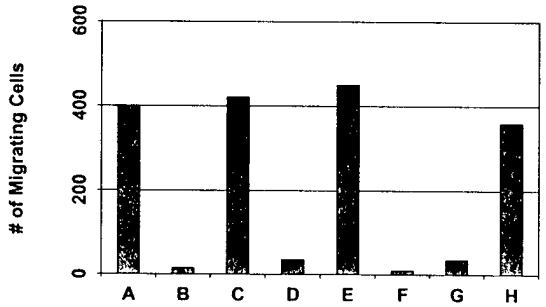

Perspective

THE GENES THAT MAKE CANCER METASTASIZE

Georg F. Weber[1*], Samy Ashkar[2]

[1]Department of Cancer Immunology and AIDS, Dana-Farber Cancer Institute,

Department of Medicine, Harvard Medical School, Boston, MA

[2]Laboratory for Skeletal Disorders and Rehabilitation, Children's Hospital,

Department of Orthopedic Surgery, Harvard Medical School, Boston, MA

[*] Address correspondence to: Georg F. Weber, Dana-Farber Cancer Institute, 44 Binney Street, Room SM 718, Boston, MA 02115. Phone: (617) 632-4629, fax: (617) 632-5446, e-mail: Georg_Weber@DFCI.harvard.edu

What are the traits that make a killer? This question has not only intrigued fans of detective stories it is also most prominent on the minds of cancer researchers. Here the characteristics of the killer are dysregulated growth control, overcoming of replicative senescence, and metastasis formation. The division of normal cells is tightly controlled by dependence on checkpoints which are pauses during the cell cycle where the fidelity of DNA replication and chromosome segregation are monitored. It is regulated by proto-oncogenes, incorporating genes for growth factors, their receptors, and associated intracellular signal transduction molecules. Antagonistic to oncogenes are tumor suppressor genes which normally provide the brakes on cell proliferation. In contrast, cancer is independent of these control mechanisms. Even with defective growth control, however, a cell could never form a tumor of substantial size because, unless it was a germline cell, it would be subject to replicative senescence, an aging process that proceeds with the number of cell divisions and in extreme cases may lead to crisis. A unique role in overcoming replicative senescence is played by the enzyme telomerase which is expressed in virtually all tumor cells but is absent from most normal cells. It prevents telomere shortening with increased number of cell divisions which would eventually cause genomic instability. Mutator genes which encode DNA repair enzymes might be more accurately referred to as meta-oncogenes because their defects give rise to mutations in oncogenes and tumor suppressor genes. Finally, most cells, with the exception of blood and immune cells, grow anchored in their microenvironment whereas cancer cells of particular tissue origin metastasize to specific target organs. The ability of cancer to disseminate throughout the body also sets it apart from benign tumors, however, the classical cancer genes conspicuously do not account for metastasis formation.

The topology of metastasis formation is mediated by the potpourri of homing receptors on the tumor cell surface and their ligands and is widely believed to have its physiologic correlate in morphogenesis during embryonic development. Unexpectedly, knockout mice in which individual genes known to participate in tumor spread were disrupted turned out to be fertile and developmentally normal (Table 1). This raises the question: What is the physiologic process that has gone astray in cancer dissemination? Despite their diversity, metastasis-associated gene products have several features in common. They comprise a set of developmentally non-essential genes which physiologically mediate stress responses, including inflammation, wound healing, and neovascularization. Consistently, the defects observed in the relevant gene targeted mice are impairments in these areas. This insight resolves some of the paradoxes of metastasis research. In contrast to morphogenesis, invasiveness and tissue damage are in keeping with the normal functions of host defense. Homing to and expansion in the lymphoid system, typically the first target in metastatic spread, corroborate the notion that cancer metastasis is based on mechanisms normally employed by immunocytes (1). Differentiation of immune cells proceeds in the context of their tissue of residence so that lymphocytes from Peyer's patches are distinct from cutaneous lymphocytes and Kupffer cells are distinct from alveolar macrophages. Recognition of topology is encoded in the relevant surface molecules and organ preference by cancer may be derived from this principle. Metastasis-associated gene products therefore constitute a unique and essential group of cancer related biomolecules whose functions are distinct from those of growth control or senescence genes.

Biologic activity of metastasis mediating gene products is extensively regulated by posttranscriptional mechanisms. Collagenases are typically secreted as precursors whose

activation requires proteolytic cleavage, collagenase type IV becomes active after cleavage by stromelysin while prostromelysin and interstitial procollagenase are activated by plasmin. Ligands for homing receptors often contain multiple domains. The heparin-binding amino-terminus of thrombospondin stimulates chemotaxis while the RGD containing carboxy-terminus mediates haptotaxis. Comparably, a prerequisite for the interaction of the N-terminal osteopontin domain with integrin receptors is phosphorylation of the cytokine while the C-terminal domain engages variant CD44 by protein-protein interaction. The gene for the homing receptor CD44 contains 10 variant exons that can be spliced into the extracellular domain and determine its engagement of various ligands. Differential effects on binding to extracellular matrix and hyaluronate also depend on the glycosylation and sulfation status of CD44. Posttranscriptional modification of function of these molecules may be beneficial in two ways. Activation by mechanisms like proteolytic cleavage or phosphorylation can be accomplished quickly in stress situations; some of the precursor molecules are widely expressed and can acutely be converted at a site of damage. Also, diversity in structure may encode organ specificity in homing and metastasis formation (a zip code of sorts).

It could be argued that metastasis-associated genes are not, in strict terms, cancer genes because mutations in them have not been linked to the risk of contracting cancer. While it is true that these genes have not yet been observed to be mutated in malignancies like the classical oncogenes (frequently through point mutations, deletions, frame shifts, or translocations) they are subject to dysregulation. A case in point is the expression of ICAM-1 on melanoma cells which is an indicator of poor prognosis. Similarly, the homing receptor CD44 is often expressed on cancer cells but not at all on their benign precursors. Alternatively, cancer cells may display

splice variants of this receptor which are not detected on their non-transformed counterparts. Therefore, aberration of genes for cancer spread occurs frequently on the levels of transcription or splicing. Without this dysregulation of gene expression tumors could not become malignant.

Like yin and yang phenomena in biology typically have a counter-balance. This holds true for the regulation of cell dissemination. Like tumor suppressor genes inhibit cell cycle progression and serve as antagonists for oncogenes, the genes that mediate metastatic spread are balanced by metastasis suppressor genes. The derived gene products typically are adhesion molecules that procure cell anchorage and inhibit migration. Expression of L-CAM is inversely correlated with the metastatic potential of various tumor cell lines. Loss of cadherin expression in squamous cell carcinomas of the head and neck, prostate cancer, and cancers of the female reproductive tract is associated with poor differentiation and high invasiveness. E-cadherin can prevent the invasive phenotype in T-lymphoma cells. Proteinases also have their antagonists. Tissue inhibitors of metalloproteinases negatively regulate invasion. Their overexpression reduces metastatic potential whereas antisense RNA enhances the malignant phenotype.

Even though uncontrolled growth does not inevitably lead to metastatic spread, consistent patterns of organ preference by cancers of particular tissue origin suggest that there is a necessary connection between mutations of oncogenes or tumor suppressor genes and the expression of genes that mediate tumor dissemination. The molecular basis for this connection is currently largely unknown. Expression of metastasis-specific splice variants of CD44 and the oncogene *ras* are connected in an autocatalytic mode in which *ras* induces promoter activity for CD44 through an AP-1 binding site while transfection of CD44v enhances the expression of *ras*. This mutual induction may contribute to the perpetuation of cell division and spreading which

are characteristic of malignancy. Motility-associated cytokines, including type IV collagenases and osteopontin, can also be induced by *ras* and similar relationships may apply for other oncogenes, including *v-mos*, *v-raf*, *v-fes* and *v-src* (2).

Recent research has identified the genes that underlie the three phenotypic characteristics of cancer and has allowed a distinction between malignant and benign tumors on the molecular level. Only tumors in which the dysregulation of growth is associated with expression of genes whose products mediate dissemination become malignant. The potential for new drug targets has emerged from the definition of molecules that are rarely expressed in the healthy adult organism. Among them are telomerase, structurally altered oncogene products such as fusion proteins or mutants, as well as some of the stress response molecules that mediate metastasis formation. Prominently, blocking the integrin $\alpha_V ß_3$, which is essential for tumor angiogenesis, has been successful in several experimental systems (3). Such progress provides the opportunity for a more successful broad attack on the cancer epidemy. As the profile of the killer becomes more refined the prospect for its containment improves.

References

1) P. Herrlich, M. Zoeller, S.T. Pals, H. Ponta H, Immunol. Today **14**, 395 (1993).

2) A.H. Greenberg, S.E. Egan, J.A. Wright, Invasion Metastas. **9**, 360 (1989).

3) W. Arap, R. Pasqualini, E. Rhouslahti, Science **279**, 377 (1998); P.C. Brooks, A.M.P. Montgomery, M. Rosenfeld, *et al.*, Cell **79**, 1157 (1994).

4) R. Schmits, J. Filmus, N. Gerwin, *et al.*, Blood **90**, 2217 (1997).

5) J. Xu, I.S. Grewal, G.P. Geba, R.A. Flavell, J. Exp. Med. **183**, 589 (1996).

6) P. Shier, G. Otulakowski, K. Ngo, *et al.*, J. Immunol. **157**, 5375 (1996).

7) A.E. May, S.M. Kanse, L.R. Lund, *et al.*, J. Exp. Med. **188**, 1029 (1998).

8) J.E. Sligh Jr, C.M. Ballantyne, S.S. Rich, *et al.*, Proc. Natl. Acad. Sci. USA **90**, 8529 (1993); H. Xu, J.A. Gonzalo, Y. St Pierre, *et al.*, J. Exp. Med. **80**, 95 (1994).

9) L. Liaw, D.E. Birk, C.B. Ballas, *et al.*, J. Clin. Invest. **101**, 1468 (1998); S. Ashkar, G.F. Weber, *et al.*, Manuscript submitted for publication.

10) J. Lawler, M. Sunday, V. Thibert, *et al.*, J. Clin. Invest. **101**, 982 (1998).

11) E.J. Kunkel, K. Ley, Circ. Res. **79**, 1196 (1996); D.S. Milstone, D. Fukumura, R.C. Padgett, *et al.*, Microcirc. **5**, 153 (1998).

12) S.D. Shapiro, Matrix Biol. **15**, 527 (1997); S.E. Dunsmore, U.K. Saarialho-Kere, J.D. Roby, *et al.*, J. Clin. Invest. **102**, 1321 (1998).

13) This study was supported by National Institutes of Health research grant CA76176 and Department of Defense breast cancer grant DAMD179818060 to GFW and Department of Defense breast cancer grant DAMD179919124 and Department of Public Health grant DPH34089930002 to SA.

Table 1: Genes that mediate cancer spread are developmentally non-essential. Cancer dissemination is induced by a group of homing receptors, their ligands and proteinases. These gene products do not play a critical role in organ development or fertility but are necessary for stress responses. (DTH = delayed type hypersensitivity, MMP = matrix metalloproteinase, uPAR = receptor for urokinase-type plasminogen activator)

TABLE 1

	gene	types of cancer	knockout mouse
receptors			
	CD44	lymphomas, sarcomas colon cancer, breast cancer	excessive granuloma formation (4)
	L-selectin	lymphoma	no DTH to cutaneous antigens (5)
	LFA-1	lymphoma	impaired immune response to alloantigens (6)
	uPAR	prostate cancer, breast cancer, gastric carcinoma, brain tumors	defect in leukocyte recruitment and adhesion (7)
	ICAM-1	melanoma, lymphoma, liver carcinoma	granulocytosis, diminished DTH, impaired neutrophil homing (8)
ligands			
	osteopontin	breast cancer, osteosarcoma	defective wound healing, absence of DTH (9)
	thrombospondin-1	breast cancer, pancreas cancer	susceptibility to pneumonia (10)
	sE-selectin	gastric cancer, breast cancer, head and neck cancer	reduced stable adhesion of leukocytes in inflamed microvasculature (11)
proteinases			
	stromelysin-3 (MMP-3)	breast cancer	impaired wound healing (12)
	matrilysin (MMP-7)	colon cancer	defective reepithelialization in wounded trachea (12)
	macrophage elastase (MMP-12)	glioma	inpaired macrophage recruitment

Customer Number: 000959

IN THE UNITED STATES PATENT AND TRADEMARK OFFICE

In re the application of Samy Ashkar and Georg Weber

Attorney Docket No. CME-121-1

For: BIOSYNTHETIC IMMUNOMODULATORY MOLECULES AND USES THEREFOR

Assistant Commissioner For Patents
Box Provisional Patent Application
Washington, DC 20231

CERTIFICATION UNDER 37 CFR 1.10

Date of Deposit: April 15, 1999 Mailing Label Number: EL266 737 834US

I hereby certify that this Cover Sheet for Filing Provisional Application (37 C.F.R. §1.51(2)(i)) and the documents referred to as attached therein are being deposited with the United States Postal Service on the date indicated above in an envelope as "Express Mail Post Office to Addressee" service under 37 CFR 1.10 and addressed to the Assistant Commissioner for Patents, Box Provisional Patent Application, Washington, D.C. 20231.

Eric J. Chesnakas
Name of Person Mailing Paper

Eric J. Chesnakas
Signature of Person Mailing Paper

COVER SHEET FOR FILING PROVISIONAL PATENT APPLICATION

Dear Sir:

The accompanying application, entitled BIOSYNTHETIC IMMUNOMODULATORY MOLECULES AND USES THEREFOR, is a provisional patent application under 37 C.F.R. §1.51(a)(2) and §1.53(b)(2).

1. ☒ The name(s) and address(es) of the inventor(s) of this application is/are as follows:

	Last Name	First Name	Middle Initial	Residence
1	ASHKAR	Samy		12 Stoneholm St., Apt 606 Boston, MA 02115
2	WEBER	Georg		
3				
4				

2. ☐ This invention was made by an agency of the United States Government or under contract with an agency of the United States Government. The name of the U.S. Government agency and the Government contract number are:

Agency: _____

Attorney Docket: CME-121-1

3. ☒ The following documents are enclosed:
   - ☒ 49 page(s) of specification
   - ☒ 13 sheet(s) of drawings
   - ☒ 3 page(s) of claims
   - ☒ 1 page(s) of abstract

4. ☐ A verified statement to establish small entity status under 37 CFR 1.9 and 1.27 is enclosed.

5. ☐ An Assignment of the invention to _____ is enclosed. A check in the amount of $40.00 for recording this assignment and a recordation form cover sheet (Form PTO 1595) are also enclosed.

6. ☒ The fee for filing this provisional application, as set forth in 37 CFR 1.16(k), is $150.00 .
   a. ☐ A check for this filing fee is enclosed.
   b. ☐ Charge the filing fee to Deposit Account No. . (A duplicate copy of this sheet is enclosed.)
   c. ☒ **The filing fee is not being paid at this time.**

7. ☐ Please charge any fee deficiencies associated with this filing to Deposit Account No. . A duplicate copy of this sheet is enclosed.

8. ☒ Please address all future communications to: **Customer Number: 000959** whose address is:

Lahive & Cockfield, LLP
28 State Street
Boston, MA 02109

and direct telephone calls to: (617) 227-7400

Respectfully submitted,

April 15, 1999
Date

Elizabeth A. Hanley
Reg. No. 33,505

LAHIVE & COCKFIELD, LLP
28 State Street
Boston, MA 02109
Tel. (617) 227-7400

BIOSYNTHETIC IMMUNOMODULATORY MOLECULES AND USES THEREFOR

Novel biosynthetic immunomodulatory molecules are provided. The biosynthetic immunomodulatory molecules include functional domains derived from osteopontin. Preferred biosynthetic immunomodulatory molecules include an IL-10 inhibitory domain derived form osteopontin. The immunomodulatory molecules of the present invention are capable of biasing an immune response in a subject to a Type 1 immune response. Accordingly, therapeutic uses are disclosed which are base on the novel biosynthetic immunomodulatory molecules of the present invention.